Agricultural Water Management 327 (2026) 110254

Contents lists available at ScienceDirect

Agricultural Water Management

journal homepage: www.elsevier.com/locate/agwat

Predictive drivers and transferability of multi-scale machine learning based crop yield prediction under drought across European and Asian climates

Hempushpa Sahu [a,b], Pradeep Kumar Garg [a], Saurabh Vijay [a], Antara Dasgupta [b,*]

[a] Department of Civil Engineering, Indian Institute of Technology Roorkee, Uttarakhand 247667, India
[b] RWTH Aachen University, Data Driven Computing Lab, Institute of Hydraulic Engineering and Water Resources Management (IWW), Faculty of Civil Engineering, Germany

ARTICLE INFO

Handling Editor - Enrique Fernández

Keywords:
Random Forest
Transfer learning
Semi-arid
Temperate
Wheat
Barley

ABSTRACT

Food security is increasingly critical due to a growing global population. Accurate crop yield prediction enables policymakers to anticipate climate shocks, such as droughts, and manage food reserves proactively. Machine learning models struggle to capture the complexity of real-world conditions, particularly during extreme events such as droughts, as these events are often underrepresented in the training data distributions, challenging predictions. This study addresses the limitation of predictability of crop yield during hydrological extremes, particularly droughts, by optimizing a Random Forest regressor using two training strategies: random and a hydrologically balanced approach. The model was applied in the Bundelkhand region in India and Germany in Europe, for wheat and barley crops. Predictions were at two spatial scales: lumped and distributed, to assess the differences in predictive drivers across scales. In Bundelkhand, for the lumped scale, the balanced approach improved Root Mean Square Error (RMSE) by 14.66 % and Mean Absolute Percentage Error (MAPE) by 29.23 % for wheat; and by 36.10 % (RMSE) and 40 % (MAPE) for barley. In Germany, the performance gains from balancing were smaller: 4.59 % (RMSE) and 6.37 % (MAPE) for wheat, with a decrease in performance for barley. The study also analyzed the spatial transferability by applying regionally trained models across sites without retraining. Results suggest that adding local features during retraining may enhance model performance in new regions. Overall, this work demonstrates the value of combining reanalysis data with ensemble machine learning for accurate crop yield prediction, offering insights to support food reserve planning and mitigate the impacts of climate extremes on food security.

1. Introduction

The growing global population necessitates enhanced food security, yet meeting the needs of nearly two billion people worldwide already presents significant challenges (Verschuur et al., 2021). Agricultural productivity is further threatened by climate extremes, such as floods and droughts, as well as compound disasters (Verschuur et al., 2021; Wan et al., 2021; Wen et al., 2023). Drought, in particular, is projected to become more frequent in the future, which is expected to enhance crop prices and threaten food security (Aalbers et al., 2023; J. Zhang et al., 2018). Accurate crop yield prediction has thus become essential for effectively planning and managing food reserves (Bellvert et al., 2025; Servia et al., 2022).

For predicting crop yields, several key climatic variables are necessary, which include precipitation, temperature, evaporation, soil moisture, humidity, solar radiation, and wind speed. In-situ data collection, traditionally used to measure these variables in the field, is both labor and cost-intensive, leading to limited spatial sampling despite the high temporal sampling rates at installed sensor locations. The ubiquity of satellite remote sensing from Earth Observation (EO) satellites has, to some extent, alleviated the spatial and temporal constraints of traditional in-situ measurements (Servia et al., 2022; Wen et al., 2023). EO

Abbreviations: EO, Earth Observation; ERA5 Land, European Center for Medium Range Forecast ECMWF Reanalysis v5; Kg/ha, Kilograms per hectare; MAPE, Mean Absolute Percentage Error; ML, Machine Learning; NDVI, Normalized Difference Vegetation Index; R^2, Coefficient of Determination; RF, Random Forest; RMSE, Root Mean Square Error; SPEI, Standardized Precipitation Evapotranspiration Index; SPI, Standardized Precipitation Index; UFZ, Helmholtz Centre for Environmental Research; U.S., United States.

* Corresponding author.
E-mail address: antara.dasgupta@rwth-aachen.de (A. Dasgupta).

https://doi.org/10.1016/j.agwat.2026.110254
Received 8 June 2025; Received in revised form 16 February 2026; Accepted 22 February 2026
Available online 26 February 2026

data can also provide spatially distributed observations of climatic variables crucial for crop yield predictions, in addition to offering other relevant crop health indicators, such as vegetation indices (e.g., the normalized difference vegetation index). But EO data does not yet exist for all climatic variables over climate time scales of more than 30 years. Therefore, researchers often use reanalysis data for land monitoring applications, drought monitoring (Gallear et al., 2025; Qian et al., 2025) and crop yield predictions (Benso et al., 2025; Yeşilköy and Demir, 2024). Reanalysis data provide a more comprehensive dataset, as they fill data gaps by interpolating in space and time, and contain lower uncertainties than model outputs or observations due to their integration via data assimilation.

Crop yield prediction is a challenging task influenced by multiple factors, including climate, topography, soil properties, water availability, and planting time (El-Kenawy et al., 2024). While traditional crop growth models have been widely used, the boom in data and cloud computing availability has shifted the focus towards machine learning (ML) for crop yield forecasting, due to expected improvements in predictive accuracy (Wang et al., 2023a). For instance, Zhuo et al. (2022) employed the WOrld FOod STudies (WOFOST) model, a process-based mechanistic model, to predict winter wheat yield in China using different input configurations. The application of data assimilation techniques within the WOFOST framework resulted in a ∼28 % improvement in prediction accuracy compared to predictions without data assimilation. Johnston et al. (2023) compared ML models as emulators of the process driven crop models, and reported a high coefficient of determination (R^2 greater than 0.95) at training locations, indicating strong predictive accuracy. However, ML models are not a universal replacement of process-based models, as their performance depends on the quality and range of input data provided to the model. Peng et al. (2020) evaluated Least Absolute Shrinkage and Selection Operator (LASSO), Ridge regression, and several ML models, such as Random Forest (RF), Support Vector Regression (SVR), Artificial Neural Networks (ANN), for yield prediction and reported that RF performed the best for predicting maize and soybean yields in the United States (U. S.) Midwest. They highlighted the benefit of using Solar Induced Chlorophyll Fluorescence (SIF) at different resolutions to improve crop yield predictions. Brandt et al. (2024) demonstrated the effectiveness of ensemble learning methods, applying meta-learning through model stacking and majority voting across six supervised ML regression estimators for three crops in Northern Germany, where majority voting outperformed others. Asadollah et al. (2024) predicted crop yield for barley, oats, rye, and wheat using remote sensing data and ML models. They applied a novel Randomized Search cross validation (RScv) approach to optimize four ensemble ML models (Gradient Boosting, Ada-boost, RF, Extra tree). For all models, RScv improved performance, with Ada-boost achieving the highest R^2 at 0.90. A review by Luo et al. (2023) suggests that advances in input data, dynamic models, and assimilation algorithms, can enhance crop yield estimation. Similarly, the review by Fares et al. (2026) highlights the importance of incorporating diverse variables such as crop management practices, soil type, and crop variety with drought indices into artificial intelligence models to improve crop yield predictions under drought conditions.

The impact of climate change on agriculture is becoming increasingly evident. Wheat, as one of the most widely cultivated staple crops, is especially vulnerable to rising temperature and shifting rainfall patterns. Gao et al. (2025) investigated the impact of climate change on winter wheat and spring wheat yield in both historical and future periods in Xinjiang, China, a semi-arid region, using five ML models: Gradient Boosting Regression (GBR), SVR, Multilayer Perceptron (MLP), Elastic Net (EN), and RF. The RF showed highest accuracy (R^2 = 0.68–0.70) for wheat yields. In contrast, future projections indicate a warming and concerning scenario, with winter wheat expected to decrease by an average of 3.9–4.8 %. These findings highlight winter wheat's sensitivity to changing climatic conditions. Comparable evidence shows declining NDVI and precipitation over time, suggesting wheat is becoming increasingly susceptible to drought stress (Su et al., 2025). Using multisource remote sensing data for rainfed wheat yield forecasting is done for Iranian provinces using Extreme Gradient Boosting (XGBoost), RF, and SVR (Bourbour et al., 2025). In Iran, climatic variables such as rainfall and temperature were found to be key variables influencing crop yield (Bourbour et al., 2025; Sharafi and Nahvinia, 2024). XGBoost performed best with 0.64 coefficient of determination. A similar study in U.S., also showed XGBoost as a better performance than RF and Linear Regression for winter wheat predictions (Khosravani Shariati and Abbasi, 2025).

ML models have been widely compared with traditional regression approaches and have generally demonstrated superior predictive performance. For example, Leng and Hall (2020) predicted maize yield in the U.S. using process-based models, a traditional multiple linear regression model, and an ML RF algorithm. They found that the ML approach explained 93 % of the observed yield variability, significantly outperforming the other methods. Similarly, Shi et al. (2024) developed SVM, ANN, RF, and linear regression models in Liaoning and Jilin, China. They tested their transferability to predict rice yield in data-sparse regions of North Korea. ML models have been applied not only to predict drought related yield losses but also to address other yield related challenges across different climatic regions. The RF model outperformed other models, even with limited training data, achieving R^2 values of 0.83–0.87. L. Li et al. (2025) developed a Knowledge-Guided Machine Learning (KGML) framework to simulate the impact of waterlogging on wheat yield in the Yangtze River Basin, China. The RF model was employed to identify changes in crop yield and to determine key features, which were subsequently utilized for uncertainty analysis. Results show that the framework demonstrates a reliable performance with an R^2 of 0.83 and RMSE of 272.3 kg/ha under waterlogging effects. Cedric et al., (2022) used three ML models, k-Nearest Neighbor (k-NN), Multivariate Linear Logistic Regression, and Decision Tree to predict the yields of six crops (banana, yams, cassava, maize, rice, and seed cotton) in West African Countries. The k-NN model outperformed the others, achieving a R^2 of 95.03 % and a Mean absolute error (MAE) of 0.160 kg/ha, with k-fold cross-validation playing a key role in hyperparameter optimization. Han and Leng, (2024) analyzed the global sensitivity of maize yield to Vapor Pressure Deficit (VPD) and used an RF model to assess the drivers of VPD changes. They found that shortwave radiation, daily maximum temperature, and minimum relative humidity account for changes in sensitivity across 72 % of the global maize-growing area. The RF model proved to be the most robust in yield prediction, demonstrating its effectiveness for handling complex environmental variables.

Despite the success in ML-based crop yield forecasting, no studies have investigated crop yield prediction capabilities of drought-induced crop yield loss, which can substantially affect both crop yields and model performance due to the extreme nature of droughts. ML models and data driven techniques are often discussed for neglecting realistic scenarios, particularly climate extremes, in training and testing datasets, leading to poor performance in out-of-distribution settings (Bowden et al., 2002; Chen et al., 2022; Kratzert et al., 2019). Incorporating a hydrologically balanced selection of training and testing data ensures the inclusion of both drought and non-drought conditions in the training and testing data splits, enabling the model to learn from more representative situations and thereby improve predictions during extremes. To the best of the authors' knowledge, no study has implemented such a balanced approach specifically for predicting crop yield under the impacts of drought, leaving a significant gap in the literature on crop yield prediction.

In this study, we specifically aim to improve crop yield predictions for drought-impacted regions, during and after drought incidents, using the power of ensemble ML, namely the RF regressor, chosen due to its ability to generalize the complex relationships that drive crop productivity. To achieve this, we utilize historical drought data from two agroclimatically diverse regions to develop a drought-informed RF regressor that predicts annual crop yield estimates, considering the impacts of drought. We also examine the effects of spatial scale on predictive accuracy and evaluate the importance of different input features across various scales and regions to understand how different causal drivers of drought influence the predictive performance of the RF model. In doing so, we answer the following research questions:

1. Does a drought-informed training strategy help improve machine learning based annual crop yield predictions?
2. Do the most important predictors of drought-induced crop yield predictions vary with different spatial scales or geographical regions with different climatologies?
3. How well does the ML-based crop yield prediction model transfer to different climatic and geographic settings?

2. Materials and methods

2.1. Study area

The study focuses on two distinct regions having different climates: Germany and the Bundelkhand region from Uttar Pradesh (UP), India. The regions were selected for their significant roles in the agricultural sector, as well as for recent drought occurrences in both, given that Germany is among the top five producing countries in Europe in 2022 (Benito-Verdugo et al., 2023), and in Bundelkhand, a majority of the population relies on agriculture for their livelihoods (Paul et al., 2021). Fig. 1 illustrates the locations and annual spatial variations in precipitation and temperature for both study sites for a drought year of 2015.

2.1.1. Bundelkhand

Bundelkhand is one of the most drought-prone areas in India. The Bundelkhand region is situated in central India, spanning latitudes 23°20′00″ N to 26°20′00″ N and longitudes 78°20′00″ E to 81°40′00″ E (Patel and Yadav, 2015), extending across two states, UP and Madhya Pradesh (MP), covering a total area of approximately 7.08 Mha. The region comprises thirteen districts: seven in UP (Banda, Chitrakoot, Hamirpur, Jalaun, Jhansi, Lalitpur, and Mahoba) and six in MP (Chattarpur, Damoh, Datia, Panna, Sagar, and Tikamgarh). We selected only the UP region of Bundelkhand as it faces frequent droughts. According to the Köppen-Geiger climate classification, Bundelkhand is characterized by a hot and semi-humid climate (Beck et al., 2018), and experiences recurrent droughts due to irregular and scant precipitation (Paul et al., 2021). It has an elevation range of 64 m to 245 m above mean sea level and receives an average annual rainfall of 800–1000 mm, with approximately 40 rainy days per year (Patel and Yadav, 2015). The air temperatures vary between 5°C and 48°C. Agriculture in Bundelkhand is predominantly rainfed (Pandey et al., 2021). The primary food production in the region is dominated by cereals, accounting for 54.6 %, followed by pulses at 32.4 %, oilseeds at 8 %, sugarcane at 0.2 %, and other crops at 4.8 % (Kundu et al., 2015).

2.1.2. Germany

Germany has a diverse agricultural landscape and spans from 47°17′00″ N to 55°00′03″ N latitudes and 5°53′00″ E to 15°2′00″ E longitudes. Germany covers a total area of 357,146 Km^2, with elevations ranging from 2962 m above sea level in the Alps to sea level at the North and Baltic Seas (Reinermann et al., 2019). According to the

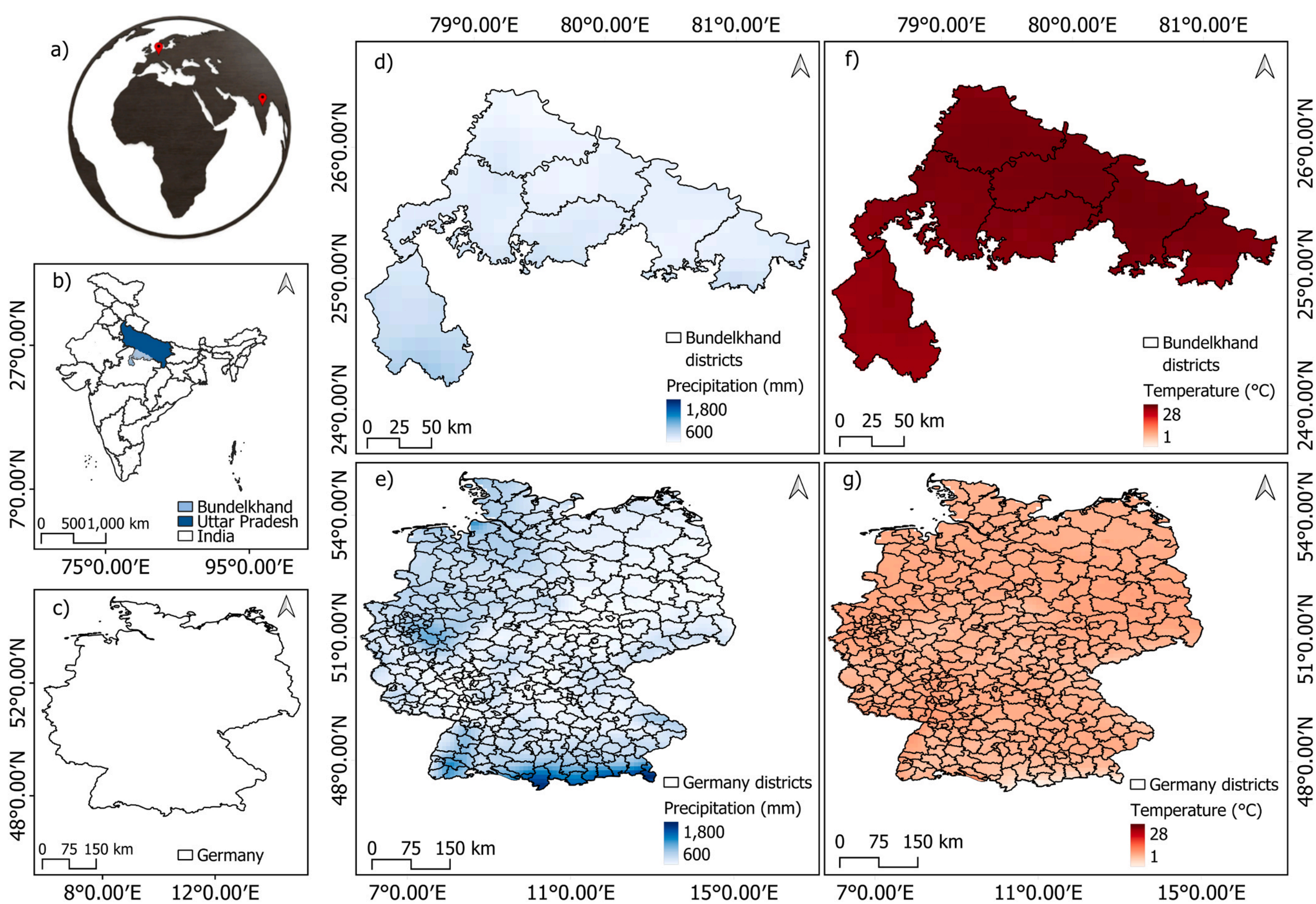

Fig. 1. Global locations of the two regions are shown in (a), with a detailed area map for Bundelkhand in (b), and Germany in (c). The spatial distribution is represented for an example drought year, 2015, with the total annual precipitation for Bundelkhand (d), and Germany (e), and the mean annual skin temperature for Bundelkhand (f), and Germany (g).

Köppen-Geiger climate classification, Germany is characterized by a temperate, humid climate with warm summers and no dry season (Blickensdörfer et al., 2022). The country's precipitation and temperature vary from north to south, resulting in substantial regional differences in weather conditions throughout the country. Eastern, northern, and western Germany is more prone to droughts, while southern Germany is affected by waterlogging (Schmitt et al., 2022). The average rainfall for June is approximately 77 mm, while in February, it is around 40 mm. The average temperature varies monthly, ranging from 0.5°C in January to approximately 17.1°C in July. Spatial variations exist, particularly in southern Germany, where the Alps influence the local climate (Blickensdörfer et al., 2022; Reinermann et al., 2019). The highest precipitation and temperatures occur during the summer months of June to August. The agricultural landscape of Germany has 71 % cropland, 28 % grassland, and about 1 % vineyards and fruit trees (Blickensdörfer et al., 2022).

2.2. Data

This study employed openly available global datasets, ensuring consistency and comparability across both study sites. A total of 14 variables were used in the study, including meteorological data, precipitation (Xu et al., 2025), temperature (Tramblay and Quintana Seguí, 2022), total evaporation (De Clercq and Mahdi, 2024), relative humidity (Sharafi and Nahvinia, 2024), soil moisture (van der Wiel et al., 2022), albedo (Lei et al., 2024), solar radiation (Sharafi and Nahvinia, 2024), and wind speed (Sharafi and Nahvinia, 2024), and a biophysical parameter Leaf Area Index (LAI) (Li et al., 2023b), and a vegetation index NDVI (Tanguy et al., 2023; Wang et al., 2023b), as well as location data such as latitude (lat) and longitude (long) (Brandt et al., 2024), were selected because they collectively capture the climate and vegetation dynamics which are essential for crop development, stress response and productivity. The study covers the period from 1990 to 2021, during which both regions experienced drought episodes, with particularly severe droughts in recent years, including 2015 in Bundelkhand and 2018 in Germany. Drought years for the Bundelkhand region were identified using district level information from official government reports (India Meteorological Department, 2020; Uttar Pradesh Government, 2023). For Germany, drought years were derived from the annual drought maps produced by the Helmholtz Centre for Environmental Research (UFZ), which provide spatially explicit estimates of drought intensity for the period 1950–2024 (UFZ-Germany n.d.). These maps represent drought conditions in the topsoil layer, defined as 0–25 cm, during the growing season from April to October, and are widely used for national scale drought monitoring. The drought type is not explicitly classified as meteorological, agricultural, or hydrological in either source. The drought intensity information was therefore used as a consistent and operational basis for defining drought years across the whole study period. While drought indices such as the SPI and the SPEI provide quantitative measures of drought severity, their calculation requires region specific choices of accumulation periods, reference distributions, and climatic baselines (Mishra and Singh, 2010; Stagge et al., 2025). These choices can vary across regions and crops, introducing additional degrees of freedom that could compromise cross-regional consistency. For this reason, externally defined drought inventories were used to ensure a uniform historical characterization of drought conditions in both study areas. For Germany, a year was classified as a drought year if any part of the country exhibited a drought intensity equal to or greater than 0.04 in the UFZ maps, reflecting the fact that the entire country was treated as a single unit in the lumped scale analysis. The threshold of 0.04 was selected based on German Drought Monitor category D1 (moderate drought), following Boeing et al. (2022), and Samaniego et al. (2013). This threshold-based approach provides a transparent and reproducible definition of drought years while retaining sensitivity to spatially heterogeneous drought conditions. Although some uncertainty is inevitable, this framework enables a consistent and comparable implementation of the balanced training strategy across both regions.

2.2.1. Climatic data

We used ERA5 Land (European Centre for Medium-Range Forecasting (ECMWF) Reanalysis v5) data, which is the fifth generation of ECMWF atmospheric reanalysis covering the globe's climate. ERA5 Land Monthly is an enhanced version of ERA5 that has been available since 1950. ERA5 Land is available globally at a spatial resolution of 0.1° with a monthly temporal resolution and is updated with a lag of 2–3 months (Muñoz-Sabater et al., 2021). Relative humidity was calculated using the ERA5 temperature at 2 m and the dew point temperature, as (Alduchov and Eskridge, 1996). Wind speed calculated from the u-component and v-component of wind available at ERA5 land monthly (P. Anais.. n.d.). A detailed description of all variables selected in the study is listed in Table 1.

2.2.2. Vegetation index and biophysical data

The NDVI data were collected from the Peking University Global Inventory Modeling and Mapping Studies (PKU GIMMS) NDVI version 1.2, which is available globally (Table 1). This dataset was generated using a Back-Propagation Neural Network (BPNN) to calibrate the GIMMS NDVI3g product using Landsat NDVI samples, incorporating explanatory variables related to spatial, temporal, and satellite information, to determine the optimal model for NDVI calibration across eight vegetation biome types. A RF fusion method was then employed to merge the Moderate Resolution Imaging Spectroradiometer (MODIS) NDVI data, extending its temporal coverage up to 2022 (Li et al., 2023a). Leaf Area Index (LAI) from ERA5 Land also serves as an indicator of vegetation greenness.

2.2.3. Crop yield data

To ensure comparability and based on data availability and crop prevalence, wheat and barley (winter crops) were selected for Bundelkhand. For Germany, the corresponding crops, winter wheat and winter barley, were chosen. Yield data are reported in kilograms per hectare (Kg/ha). The data sources are listed in Table 1, while Table 2 outlines the selected districts from the study areas in both regions.

2.3. Methods

This study employs the ensemble machine learning model Random Forest Regressor to predict crop yield, additionally providing insights on agricultural droughts. Fig. 2 illustrates the methodology used in the paper. RF is a supervised learning model used for classification and regression analysis (Breiman, 2001), which constructs a forest of decision trees during training, and outputs are based on mean prediction from the individual trees in case of regression and a majority voting in case of classification. The randomness of feature selection from each subset of the decision trees helps it manage outliers and noisy data effectively, reducing the risk of overfitting, especially when dealing with limited training data (Baig et al., 2024).

2.3.1. Feature selection

Feature selection is a crucial step in machine learning as it removes redundancy by preventing the selection of highly correlated features, thereby reducing overfitting and improving model efficiency (Shahhosseini et al., 2021). Although, RF model can handle predictors with high multicollinearity, including them may introduce noise and uncertainty into the algorithm, which affects variable importance rankings (Mahdizadeh Gharakhanlou and Perez, 2024). For this reason, we conducted a Pearson correlation test on 22 features (Figure A1), although this only detects linear correlation among the data whereby non-linear correlation between the variables may be missed. After filtering highly correlated features, we also considered their unique physical contributions to the crop yield prediction problem such that

Table 1
Description of all input and target variables used in the analysis, including their units, spatial and temporal resolution, rationale for inclusion, and data sources.

Variable (name in this study)	Unit	Spatial resolution	Temporal resolution	Reason	Source
Crop yield - Bundelkhand	Kilograms/ hectare	District wise	Seasonal	Proxy for agricultural drought	(ICRISAT-District Level Data n.d.) (1990–1996) and (DES | Area, Production & Yield - Reports, n.d) (1997–2021)
Crop yield - Germany	Kilograms/ hectare	District wise	Annual	Proxy for agricultural drought	(Duden et al., 2024)
Skin temperature (skin_temp)	K converted to °C	0.1 °	Monthly	Increased temperature enhances evaporation, thereby reducing soil water and affecting crop maturity	ERA5 Land (ERA5-Land monthly averaged data from 1950 to present, n.d.)
Surface net solar radiation sum (solar_radiation)	J/m^2			Influences transpiration, and so if water availability is limited, it can lead to crop losses	
Total evaporation (total_evapo)	m of water equivalent			Increased evaporation deteriorates the soil water condition and crop health	
Relative humidity (from dew point temperature 2 m and temperature 2 m) (rel_hum)	%			It can reduce moisture in the air, increase evaporation, and potentially cause water stress in crops	
Forecast albedo (for_albedo)	%			High albedo can reduce the water storage capacity of soils	
Total precipitation sum (total_precip)	m			Provides soil moisture, thus strengthening the root zones	
Volumetric soil moisture layer 1 (vol_sm_1) (0–7 cm)	Volume fraction			Important during early growing periods, as it influences soil temperature and evaporation	
Volumetric soil moisture layer 2 (vol_sm_2) (7 −28 cm)	Volume fraction			Holds the majority of the active root system, supporting early to mid-plant growth	
Volumetric soil moisture layer 3 (vol_sm_3) (28–100 cm)	Volume fraction			Necessary for crop maturity during dry periods, such as droughts	
Wind speed (from the u-component of wind 10 m and the v-component of wind 10 m) (wind _speed)	m/s			High wind may dry the air, and evaporation increases with wind speed	
Leaf area index high (lai_h)	Area fraction			Indicator of vegetation coverage	
NDVI (mean_ndvi)	Unitless	0.0833 °	Bi-monthly	The indicator of greenness, if low, suggests potential issues affecting the crops	PKU GIMMS NDVI (Muyi Li et al., 2023)

Table 2
Number of districts included from Bundelkhand and Germany for the full study period from 1990 to 2021, showing total district counts and the subsets with complete yield records for wheat and barley used in the analysis.

Common crops	Total number of districts in the study area		No. of the districts with yield data for the complete study period for the selected crop		No. of districts with both wheat and barley yield data for the study period	
	Bundelkhand	Germany (Duden et al., 2024)	Bundelkhand	Germany	Bundelkhand	Germany
Wheat	7	397	5	242	5	201
Barley	7	397	5	219		

some correlated features were still retained due to this additional information they incorporate. Some variables such as total precipitation, volumetric soil moisture layers, solar radiation, and relative humidity exhibit high linear correlation due to mutual influence. Nevertheless, we retained them, assuming they provide distinct information to the model in addition to the correlated redundant information. Since the objective is to predict a continuous variable while retaining all relevant and distinct land surface information, we chose not to remove certain features. Feature selection was based on correlation analysis and expert judgment. This process produced 12 independent features excluding latitude and longitude, for annual-scale crop yield predictions using RF. Latitude and longitude were excluded from the correlation test, as the formula of Pearson correlation is the covariance of two variables divided by the product of the standard deviation of the two variables, which results in undefined values due to a standard deviation value equal to zero.

2.3.2. Training and testing

In machine learning, data is typically split into training and testing sets, allowing the model to learn from a portion of data and validate its performance on the remaining data (Jhajharia et al., 2023; Seyedmohammadi et al., 2024). We allocated 90 % data for training and 10 % for testing as per the peer-reviewed literature (e.g., Akbari et al., 2025; Asfaw et al., 2025; Cedric et al., 2022; Hauswirth et al., 2021). For this study, we trained the model in two different scenarios - random selection and a hydrologically balanced selection. Random selection does not guarantee a balanced representation of drought and non-drought years scenarios, while hydrologically balanced ensured this in both training and testing.

2.3.3. Parameter optimization

Hyperparameter tuning is crucial for optimizing the model performance (Mahdizadeh Gharakhanlou and Perez, 2024; Sánchez et al., 2025; Zhao et al., 2019). However, default settings in the RF model often produce reliable results (Garg et al., 2024). In this study, we performed parameter optimization using the hyperparameters listed in Table 3. *GridSearchCV* was used to identify the optimal parameter set and optimize evaluation metrics (Shahhosseini et al., 2021; Xu et al., 2025).

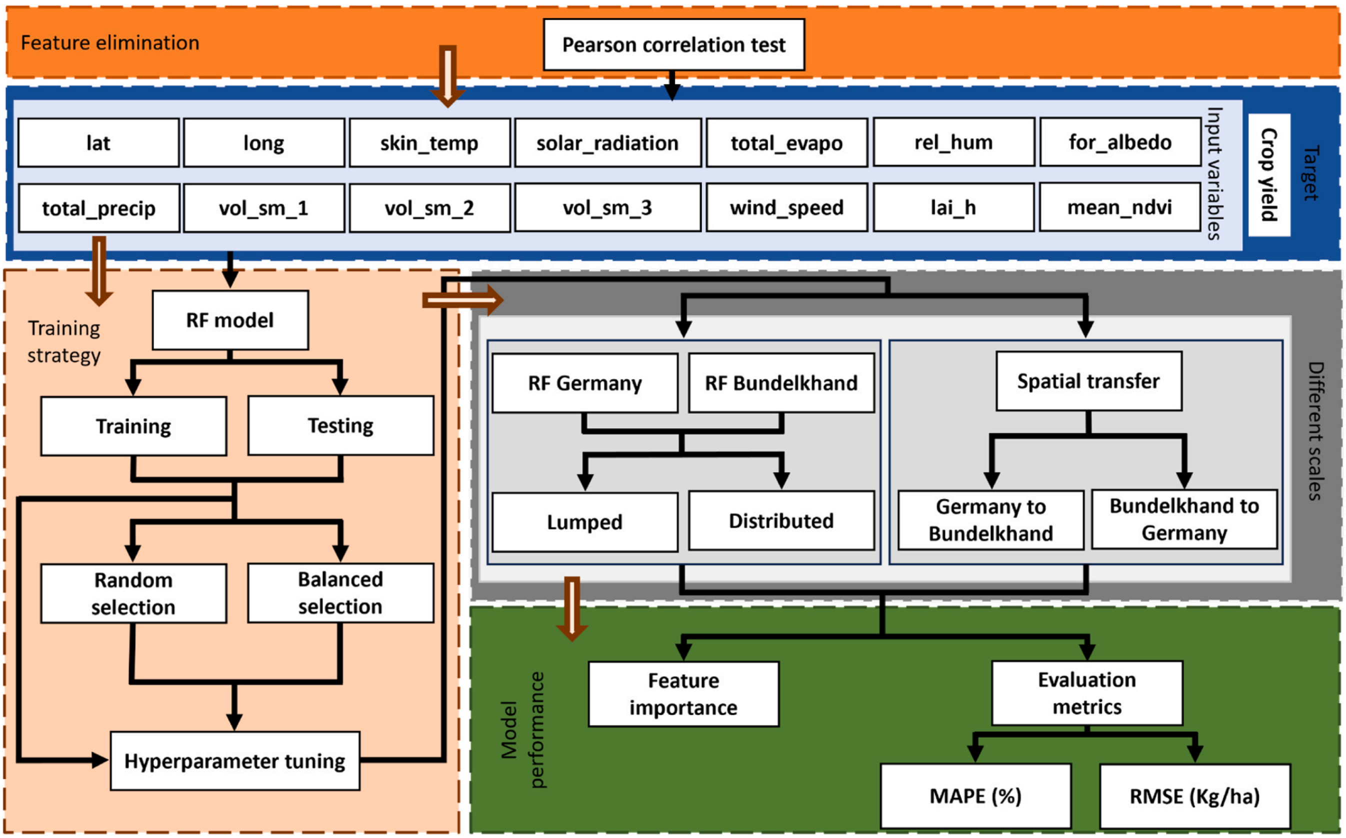

Fig. 2. Overview of the modeling workflow, showing data selection and feature elimination, followed by Random Forest training, feature importance analysis, and model performance evaluation.

Table 3
Random Forest hyperparameters evaluated during model tuning, including their definitions and the values tested in this study.

Hyperparameter	Definitions	Used in the model
'n_estimators'	the value of the number of trees it will grow, default value: 100	100, 200, 300
'max_depth'	denotes the maximum depth of the trees, default value: None	None, 10, 20, 30
'min_samples_split'	minimum number of samples required to split a node. It can be int or float	2, 5, 10
'min_samples_leaf'	the minimum number of samples required to be at a leaf node. It can be int or float	1, 2, 5
'bootstrap'	whether bootstrap samples are used when building trees. If False, the whole dataset is used to build each tree.	True, False

GridSearchCV conducts exhaustive searches over all specified hyperparameter combinations to maximize model performance. A five-fold cross-validation was applied to assess predictive accuracy to reduce data split randomness, reduce overfitting, and enhance generalization (Ennaji et al., 2025; Maier et al., 2023; Roberts et al., 2017; Sweet et al., 2023; Tegegne et al., 2017).

2.3.4. *Feature importance and spatial variations*

Feature importance analysis helps identify the most influential variables in the model by ranking them based on their contribution to the target (e.g. crop yield in this study) prediction. In the RF model, two methods of feature importance analysis are 'Mean Decrease in Impurity (MDI) based on total variance (squared error)' and 'Permutation Importance'. The permutation importance ranks features based on performance changes after shuffling the features. In this study, we applied the variance reduction method where the mean decrease in impurity is calculated based on the reduction in mean squared error (MSE) at each split across all trees. The greater the decrease in impurity, the more important the feature (Joshi et al., 2023). It is important to note that highly correlated features can affect feature importance rankings, as the model may prioritize one feature over another. As a result, some features with high correlation may appear less significant in the final analysis.

Here, we carried out lumped (a single model for all districts) and distributed (district-wise models) analyses for studying large scale and fine scale spatial variations, respectively. In large-scale analysis, data from the entire study sites (separately for Bundelkhand and Germany) was provided as input, and a single model was used to evaluate the overall performance of the variables throughout the region. In contrast, the fine-scale analysis involved training separate models at the district (sub-region) level, allowing for a detailed examination of key features specific to each district as well as a comparison of predictive performance.

2.3.5. *Spatial transferability*

Given the study focuses on two diverse agricultural regions, we did the transferability of the models to investigate whether the model is transferable as is or needs retraining with local data. The model was first trained at one location and tested on the other by simply running inference, and vice versa. This method helps assess the model's predictive capability across different regions since crop productivity is highly influenced by climate and local topography. This test was crucial for evaluating the model's adaptability towards varying geographic conditions.

2.3.6. *Evaluation metrics*

Here, we considered Root Mean Square Error (RMSE) and Mean

Absolute Percentage Error (MAPE) for model performance assessment (Nevavuori et al., 2019; van Klompenburg et al., 2020). Since we wanted to analyze both absolute (RMSE) and relative errors (MAPE), we used these metrics, which are also widely used in regression analysis (Ansarifar et al., 2021; El-Kenawy et al., 2024; Khechba et al., 2025; Mahdizadeh Gharakhanlou and Perez, 2024; Saravanan and Bhagavathiappan, 2024; Y. Zhang et al., 2025). RMSE is calculated as the squared difference between the predicted and the observed values. The RMSE value may vary from 0 to ∞ , and the optimum value is between 0 and 1. The lower the RMSE, the better the prediction. MAPE is calculated as the percentage of the difference between predicted and observed values. Lower values of MAPE indicate higher accuracy.

3. Results

3.1. Impact of different model training strategies

3.1.1. Lumped (Large-scale) analysis

This section reports lumped scale results using a single model for all districts. Table 4 shows performance changes for both training approaches across the two crops. In Bundelkhand, the hydrologically balanced selection strategy produced better results (see Table 4) than the random selection strategy for both barley and wheat. Both random and balanced strategies yielded comparable results in case of Germany. However, the model overall performed better in Germany as compared to Bundelkhand. While training the model we also did hyperparameter tuning to optimize the model. The best hyperparameters for each model are shown in the supplementary section. Table S1 provides best parameters of the model for lumped scale analysis for both crops in Bundelkhand, and Table S2 for Germany for hydrologically balanced approach.

3.1.2. Distributed (District-wise) analysis

This section reports the results of a distributed prediction; Table 5 shows the change in performance. The visualization of the evaluation metrics for both crops from hydrologically balanced approaches are shown in Fig. 3 as violin plots for both regions. In Bundelkhand, the limited number of districts results in less pronounced variability. Wheat shows lower prediction errors compared to barley, both in terms of MAPE and RMSE. In Germany, RMSE and MAPE values are concentrated in the central range but also display a widespread, suggesting the presence of possible outliers, likely influenced by a higher number of districts. Same set of hyperparameters were tuned for district wise predictions also, the best hyperparameters found are listed in Table S3 and S4 for wheat and barley in Bundelkhand and Table S5 and S6 for wheat and barley in Germany for hydrologically balanced approach.

3.2. Feature importance analysis

3.2.1. Lumped (Large-scale) analysis

Fig. 4 presents the Pearson correlation plot of Bundelkhand and Germany, while Fig. 5 displays the combined feature importance for wheat and barley across both regions. Feature importance is derived using the hydrologically balanced selection approach, which demonstrated superior performance (see Table 4). The correlation heatmap highlights interdependence among variables. Notably, some features were retained despite strong correlations (See Section 3.1.1 and Figs. 4(a), 4(b)). Examining these correlation values helps understand the feature rankings within the model, since feature correlations can lower the importance observed via the variance reduction, as the model simply picks a different correlated feature to rely on internally for the prediction.

In Bundelkhand, the most influential features (Fig. 5) for wheat were NDVI, albedo, and evaporation, followed by latitude, despite the relatively small variation in the region's latitude (23°20′00″ N to 26°20′00″ N). Solar radiation, temperature, relative humidity, precipitation, wind speed and soil moisture layers follow in decreasing order of importance. From Fig. 4(a), solar radiation, relative humidity and temperature are seen to be highly correlated with precipitation and soil moisture layers. Even in cases where relative humidity and the first soil moisture exhibit approximately 90 % correlation, the remaining uncorrelated component still provides additional independent information that contributes to the model's predictive performance. However, the soil moisture layer had minimal influence on the yield predictions for wheat. A notable difference in feature importance was observed for barley, with the soil moisture layer 3 ranking fourth and precipitation fifth, unlike in wheat, indicating differences in key features between the two crops.

In Germany, key predictors (Fig. 5) for wheat include latitude, longitude, albedo, NDVI, precipitation, temperature, evaporation, and solar radiation. For barley, important features are latitude, evaporation, longitude, temperature, solar radiation, albedo, precipitation, and NDVI. Leaf area index, which primarily indicates vegetation greenness, ranked lower in importance. In Fig. 4(b), a strong correlation between precipitation and humidity may have influenced the humidity ranking for both crops wheat and barley.

3.2.2. Distributed (District-wise) analysis

Fig. 6 shows the feature importance distribution using box and whisker plots for both crops in Bundelkhand and Germany. The box in the plot shows the maximum value concentrated in that range. The median value of each feature is differently aligned indicating skewness of the values in that feature. Latitude and longitude are not included in the list as in the distributed model it did not show any importance.

For Bundelkhand, with only five districts, the box plots show a concentrated data without outliers. The rankings of features be like those observed in Germany, with NDVI emerging as the most important feature across all districts for wheat and for three districts in barley of Bundelkhand. For other features such as evaporation, solar radiation, skin temperature, and relative humidity the visible spread (Fig. 6, see Bundelkhand crops) indicates that different districts assign varying levels of importance to these factors. For barley, wind speed, humidity, and soil moisture (layer 3) ranked among the top features in one district each. Unlike wheat, barley was more dependent on soil moisture (layer 3) (28–100 cm) rather than shallower layers. In Bundelkhand (Fig. 4(a)), humidity exhibited a stronger correlation with soil moisture layer 1 and layer 2 as compared to layer 3. This suggests a possible dilution of

Table 4
Model performance for wheat and barley yield prediction in Bundelkhand and Germany at the lumped spatial scale under two training strategies. Random selection denotes unconstrained random sampling of years into training and testing sets, while balanced selection denotes a hydrologically informed split in which both drought and non-drought years are represented in each set. Performance is reported using Root Mean Square Error (RMSE) and Mean Absolute Percentage Error (MAPE). The percentage change indicates the relative improvement or deterioration of the balanced strategy compared with the random strategy.

Crop	Location	Random selection		Balanced selection		Percentage drop	
		RMSE (Kg/ha)	MAPE (%)	RMSE (Kg/ha)	MAPE (%)	RMSE (Kg/ha)	MAPE (%)
Wheat	Bundelkhand	490.97	21.76	418.97	15.40	(+) 14.66 %	(+) 29.23 %
Barley		668.66	43.77	427.24	26.26	(+) 36.10 %	(+) 40.00 %
Wheat	Germany	659.12	7.69	628.85	7.20	(+) 4.59 %	(+) 6.37 %
Barley		666.56	8.67	681.85	8.73	(-) 2.29 %	(-) 0.69 %

Table 5
Model performance for wheat and barley yield prediction in Bundelkhand and Germany at the distributed (district) scale under two training strategies. Random selection denotes unconstrained random sampling of years into training and testing sets, while balanced selection denotes a hydrologically informed split in which both drought and non-drought years are represented in each set. Performance is summarized using the median Root Mean Square Error (RMSE) and Median Absolute Percentage Error (MAPE) across districts. The percentage change indicates the relative improvement or deterioration of the balanced strategy compared with the random strategy.

Crop	Location	Random selection		Balanced selection		Percentage drop	
		Median RMSE (Kg/ha)	Median MAPE (%)	Median RMSE (Kg/ha)	Median MAPE (%)	Median RMSE (Kg/ha)	Median MAPE (%)
Wheat	**Bundelkhand**	670	41.44	577.49	18.52	(+) 13.81	(+) 55.31
Barley		620	41.34	832.77	34.69	(-) 34.32	(+) 16.09
Wheat	**Germany**	710	7.63	800.64	9.65	(-) 12.77	(-) 2.65
Barley		950	11.93	724.75	9.52	(+) 23.71	(+) 21.33

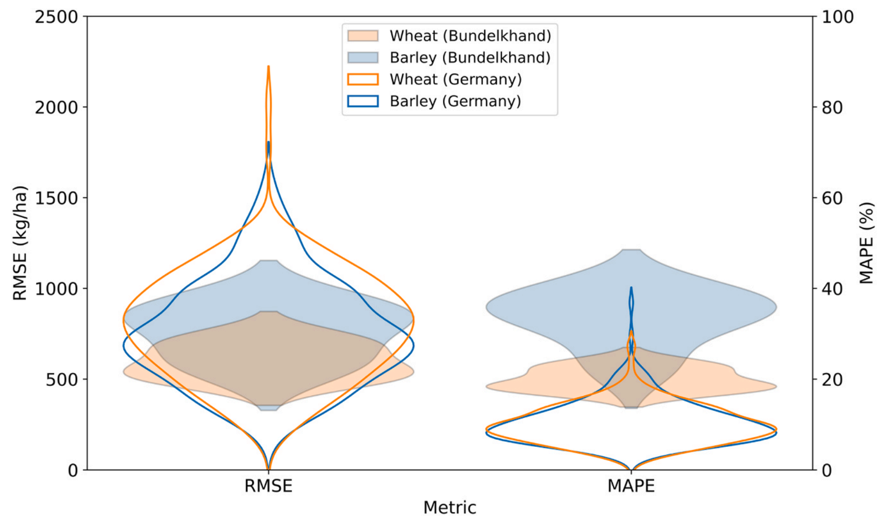

Fig. 3. Violin plots of Root Mean Square Error (RMSE) and Mean Absolute Percentage Error (MAPE) for wheat and barley in the different districts of Bundelkhand and Germany under the hydrologically balanced training strategy.

importance between these features, possibly leading to a transfer of importance between features. It is also possible that the high correlation between soil moisture layers may also prevent precise ranking of their individual feature importance (see correlation map Fig. 4).

In Germany, NDVI emerges as the most important feature for more than 80 districts for both wheat and barley, with consistent importance and minimal outliers. Following NDVI, key features include evaporation, solar radiation, and temperature, all ranking at top places across multiple districts. Other features, such as precipitation, humidity, wind speed, and soil moisture (layer 3), are the most important for crop yield prediction only in specific areas. Since solar radiation is highly correlated with precipitation, soil moisture layers, and humidity, the importance is distributed across these features. As a result, other features receive a lower ranking (Fig. 4(b)). In Germany, more outliers are observed in all features.

3.3. Spatial transferability

To assess the transferability of the model across regions, for crop yield prediction the model was first trained in one location and tested in another location and vice-versa on a lumped scale. This evaluation used datasets of varying volumes as Bundelkhand has 5 districts, and Germany has 201 districts which are two distinct regions within the study.

The results of the model transfer are presented in Tables 6 and 7. The first case evaluates model transfer from Bundelkhand to Germany, where the model produced satisfactory results, with only a minor relative error difference of 1.36 % higher than wheat (Table 6). In comparison, the second case applies the model from Germany to Bundelkhand and shows less acceptable results in terms of relative error (MAPE). Interestingly, the RMSE values in both transfer scenarios do not differ substantially with 1.71 % absolute difference in case of wheat and 1.79 % for barley (Tables 6 and 7). Nevertheless, the results indicate that the model requires retraining, likely due to the differing climate conditions and data availability between the two regions. Overall, the transfer from Bundelkhand to Germany performed better than the transfer from Germany to Bundelkhand.

4. Discussion

4.1. Selection of training strategy

The RF model has been extensively used in the past for crop yield predictions, typically relying on random splitting of data into training and testing sets. However, the choice of training strategy is crucial, since the effectiveness of data splitting depends on how well the splits represent real-world hydroclimatic conditions. To address this, we implemented a hydrologically balanced selection strategy that explicitly accounts for both drought and non-drought years, ensuring that these conditions are represented in the training and testing datasets. However, it should be noted that the choice of drought classification and the selected drought year may affect model performance, as observed in both of our study regions. The balanced selection improved the model performance in the Bundelkhand region, while in Germany, the impact was less pronounced. This difference is likely related to regional variations in yield drivers (Schmitt et al., 2022) and the underlying distribution of drought and non-drought years. Benito-Verdugo et al., (2023) reported that wheat and barley yields in Bayern, Germany, increased by approximately 11 % even during drought periods. Consistent with this

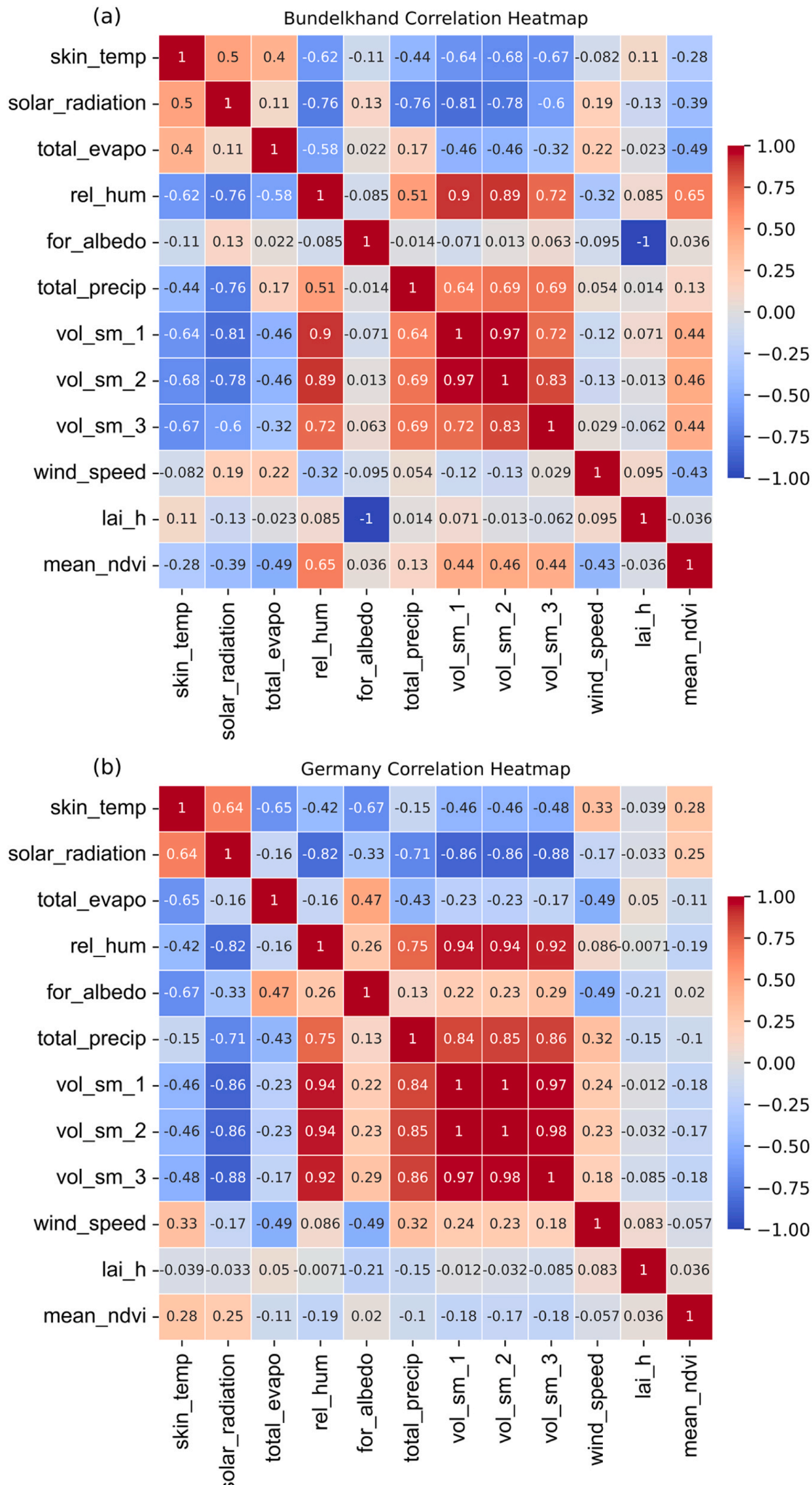

Fig. 4. Pearson correlation matrices of the selected model input variables for (a) Bundelkhand and (b) Germany.

finding, our results show that for Germany, the balanced data split resulted in a slight decline in predictive performance for barley (Table 4), suggesting that yield variability in the region is not primarily driven by drought (Benito-Verdugo et al., 2023). In our German dataset, 23 of the 32 study years were classified as drought years (refer to Supplementary file), leaving only a small number of non-drought years. Consequently, the balanced approach closely approximates a random split and therefore does not show a performance advantage over Bundelkhand. In contrast, Bundelkhand has only 10 identified drought years, which may have resulted in uneven representation between the

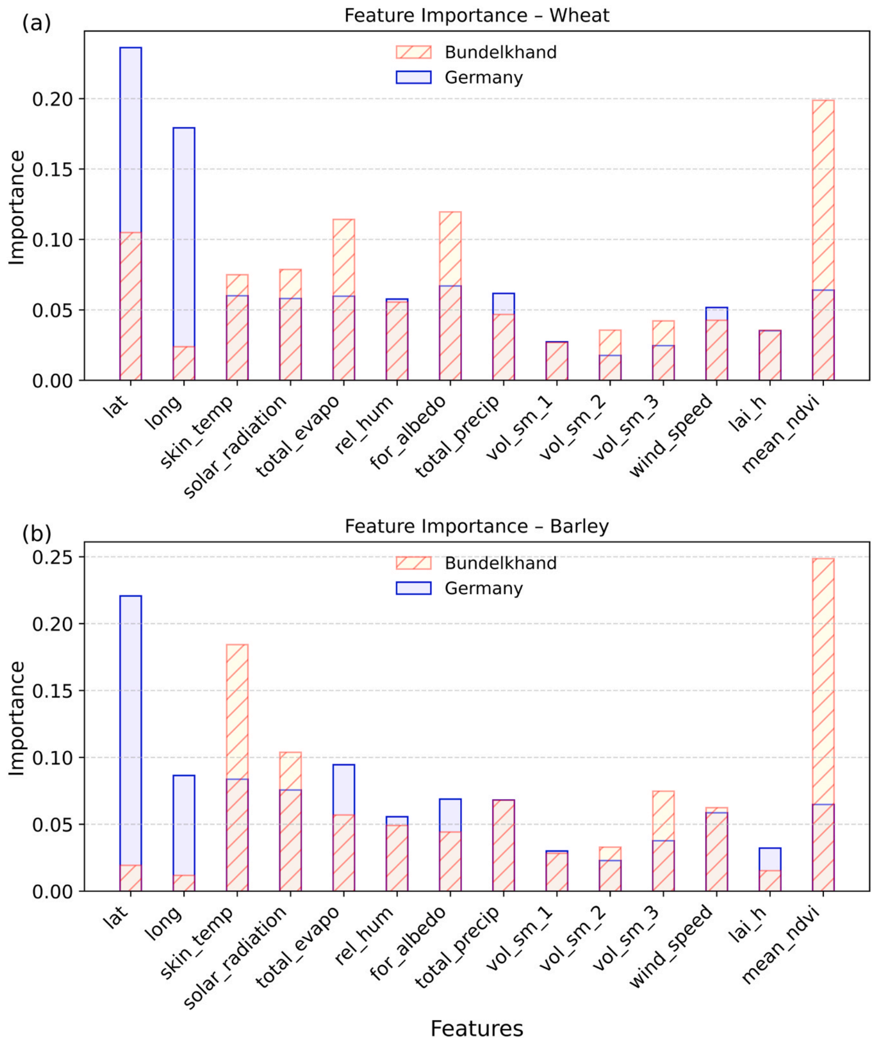

Fig. 5. Feature importance for (a) wheat and (b) barley in Bundelkhand and Germany, estimated using the mean decrease in impurity from the Random Forest models.

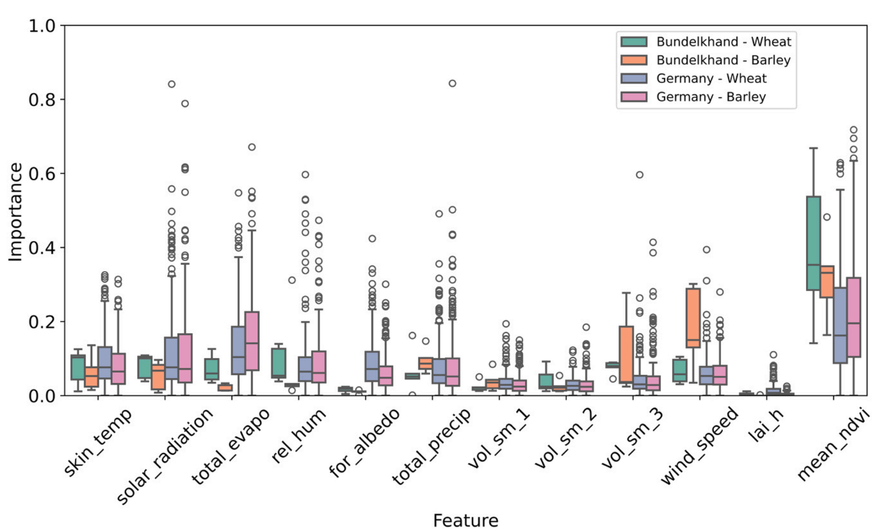

Fig. 6. Box-and-whisker plots of district-level feature importance for wheat and barley based on mean variance from the Random Forest models. The boxes indicate the interquartile range, the central line denotes the median, and the whiskers represent the data range, with outliers shown as circles. Latitude and longitude are omitted because they did not exhibit importance variations in the distributed-scale analysis due to limited variability within districts.

training and testing sets using the random approach. The balanced approach, therefore, provided a more representative data partitioning,

Table 6
Performance of spatial transfer from Bundelkhand to Germany for wheat and barley, reported using Root Mean Square Error (RMSE) and Mean Absolute Percentage Error (MAPE).

	RMSE (Kg/ha)	MAPE (%)
Wheat	4421.05	59.22
Barley	4055.01	60.03

Table 7
Performance of spatial transfer from Germany to Bundelkhand for wheat and barley, reported using Root Mean Square Error (RMSE) and Mean Absolute Percentage Error (MAPE).

	RMSE (Kg/ha)	MAPE (%)
Wheat	4345.61	213.51
Barley	4127.77	277.96

which likely resulted in a notable improvement in model performance for this region. This highlights the importance of ensuring that training and testing datasets reflect the full range of hydroclimatic conditions, particularly when analyzing extreme events such as droughts, as this leads to more reliable and robust model performance (Arsenault et al., 2018; Chen et al., 2022; Hauswirth et al., 2021; Tegegne et al., 2017; Zhou et al., 2025). In environmental and hydrological machine learning, the choice of data partitioning has been shown to strongly influence model performance and interpretation, particularly in systems characterized by regime shifts and extremes (Arsenault et al., 2018; Asfaw et al., 2025; Hauswirth et al., 2021). Model tuning was further stabilized through five-fold cross-validation within the training set during hyperparameter optimization, which reduces sensitivity to any single partition and limits overfitting (Maier et al., 2023; Sweet et al., 2023; Tegegne et al., 2017).

4.2. *Influencing variables*

To accurately predict crop yield and derive meaningful insights for future management, it is essential to understand the key variables that influence it. Thus, we conducted a feature importance analysis using the mean decrease in impurity, based on variance reduction of the mean squared error. In the case of lumped-scale predictions, location-related variables such as latitude and longitude emerged as significant predictors. This finding is consistent with Brandt et al. (2024) who found longitude to be a key factor in wheat yield estimation in Germany, while meteorological variables were comparatively less influential. A similar pattern was reported by X. Li et al. (2024), where adding temperature and precipitation did not enhance the predictive performance of the model. However, Cai et al. (2019) observed that while climatic data can complement remote sensing data in yield predictions, satellite-derived variables (e.g., NDVI) were still more important to the yield prediction model than climatic variables (e.g., precipitation), supporting our findings. In both regions, NDVI captured the most information, followed by solar radiation, evaporation, and temperature (Han and Leng, 2024; Ruan et al., 2022; Sahu et al., 2025a). These variables already captured much of the relevant variability, which explains precipitation and soil moisture, being highly correlated with them; were assigned a lower importance score. Solar radiation also appeared as one of the top important features for both crops in both regions, which corroborates the results of Webber et al. (2020), who found photosynthetically active radiation as the most important to capture yield losses for wheat and barley across several regions in Germany, particularly for the 2018 drought period. Feature importance varies between crops and regions (Figs. 5(a) and 5(b), Fig. 6) (Li et al., 2023b; Sahu et al., 2025b), and the features should be checked for multicollinearity before being provided as input to the model (Schwarz et al., 2020). Because Germany spans a wide range of climatic regions and has many districts, the distribution of feature importance values across districts is broader, and the presence of outliers is expected. Conversely, in Bundelkhand, with fewer districts, exhibits narrower distributions of feature importance across variables.

4.3. *Spatial transferability*

We evaluated the spatial transferability of the RF models to assess their applicability across regions using lumped scale predictions. Model performance under spatial transfer was generally weak, which can be partly attributed to the large imbalance in available training data between the two regions, with 201 districts in Germany and only 5 in Bundelkhand. As shown by Khan et al. (2024), the performance of transferred models strongly depends on the amount of training data available. This indicates the need for retraining and fine-tuning with the incorporation of local data to improve model adaptability and prediction accuracy. In addition, differences in climate and phenology between the two regions likely contributed to the limited transferability, as also reported by (Orynbaikyzy et al., 2022). Previous studies explored transferability in different contexts. For instance, Hoppe et al. (2024) used machine learning based transfer learning for crop classification across multiple spatial, temporal, and phenological scenarios, demonstrating that sufficient local data, in terms of both quality and quantity, is essential to achieve robust cross-regional transfers. Similarly, Khan et al. (2024) used a deep transfer learning model for crop yield prediction in the U.S. that considered spatial and crop level transfer and obtained reasonable performance. However, they also emphasized that yield prediction remains challenging due to differences in climatic and crop growth patterns. Thus, we have different feature importances for wheat and barley, as well as for Bundelkhand and Germany. The combined effect of regional heterogeneity and the complex dynamics of drought therefore provides a plausible explanation for the limited performance of spatially transferred models, as also observed by other studies (e.g., (B. Zhang et al., 2023).

4.4. *Strengths and limitations*

A key strength of the study is the use of a relatively simple RF model combined with a hydrologically informed training strategy, which ensures an appropriate and representative split between training and testing data. By emphasizing data representation, the modeling framework is designed to reflect real world hydroclimatic variability. The RF algorithm was selected for its robustness, its ability to limit overfitting, and its reliable performance with comparatively small datasets, making it suitable for predictions under extreme conditions, such as drought (Bourbour et al., 2025; Dangare et al., 2026).

Despite the robustness of the proposed methodology, certain limitations must be acknowledged in the study design. The model was evaluated within a limited spatial context, which may restrict its generalizability. Testing across multiple regions with varying climatic conditions is necessary to confirm the broader applicability of this approach. Additionally, the current dataset is based on climatic and biophysical variables. It does not account for several region-specific factors that influence crop yield, such as soil properties, topography, and irrigation infrastructure, which may impact the accuracy of yield predictions. Furthermore, the study is limited to open-source reanalysis and satellite-based datasets; no in-situ observations were incorporated into the analysis.

Here, drought years were identified using external drought inventories widely adopted by national and international agencies (India Meteorological Department, 2020; UFZ-Germany n.d.; Uttar Pradesh Government, 2023) which enabled a consistent historical characterization of drought conditions across the whole study period. While drought indices like SPI and SPEI provide valuable quantitative measures of drought, this study emphasizes evaluating the impact of a drought-informed training strategy based on externally defined drought classifications, rather than considering them as inputs. Future work could extend the present framework by incorporating indicators such as the SPI and SPEI, together with region specific variables including soil properties, terrain, and irrigation, to examine how additional sources of information further enhance predictive skill.

5. Conclusions

In this study, we evaluated an ensemble Random Forest model for predicting crop yields, with a particular focus on drought-induced losses, across two spatial scales - lumped and distributed. A novel training approach was employed, comparing two approaches - random and hydrologically balanced selection. To enhance predictive accuracy, hyperparameter tuning was performed. We also assessed spatial transferability to evaluate the model's ability to adapt across different regions. Our results show that applying an appropriate (balanced) training strategy can notably improve the model's performance. However, for Germany, the difference between the training strategies was minimal with random splits performing marginally better, since a high proportion of drought years meant that the balanced data split closely resembled the random split. We also examined the importance of various features using variance reduction within the RF framework. We identified the Normalized Difference Vegetation Index as the most influential predictor for both crops, across spatial scales and regions, followed by solar radiation, evaporation, and temperature. The model performance was limited when transferred spatially, indicating the need for local retraining. This study offers a first robust assessment of crop yield predictions under drought conditions using openly available and globally consistent EO and reanalysis datasets using an ensemble ML model. Models developed herein pave the way for anticipatory action to reduce the impact of drought-induced crop losses in data scarce regions, ultimately reducing global climate-related shocks to food security.

Funding

This research received no external funding.

Appendix

CRediT authorship contribution statement

Hempushpa Sahu: Writing – review & editing, Writing – original draft, Visualization, Validation, Software, Methodology, Investigation, Formal analysis, Data curation, Conceptualization. **Pradeep Kumar Garg:** Writing – review & editing, Supervision, Resources, Conceptualization. **Saurabh Vijay:** Writing – review & editing, Supervision, Resources, Conceptualization. **Antara Dasgupta:** Writing – review & editing, Supervision, Resources, Methodology, Data curation, Conceptualization.

Declaration of Generative AI and AI-assisted technologies in the writing process

During the preparation of this work, the authors used ChatGPT to improve language and readability. After using this tool, the authors reviewed and edited the content as needed and take full responsibility for the content of the publication.

Declaration of Competing Interest

The authors declare that they have no known competing financial interests or personal relationships that could have appeared to influence the work reported in this paper.

Acknowledgments

The authors acknowledge the support from the Ministry of Education, Government of India, for providing Ph.D. scholarship and Advanced Research Opportunities Program (AROP) scholarship received from RWTH Aachen University, Germany, as a guest researcher at the Data Driven Computing Lab of the Faculty of Civil Engineering.

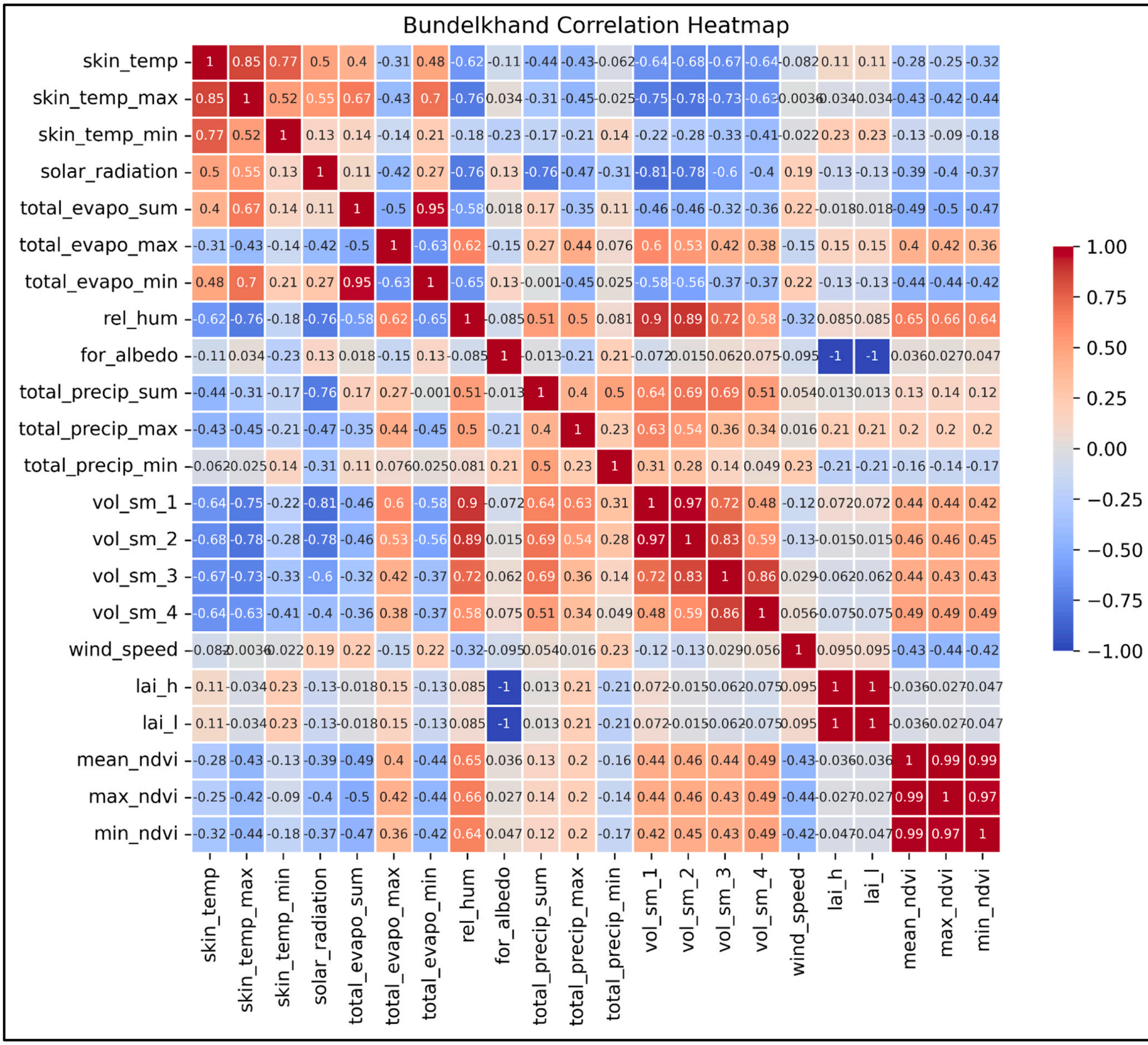

Figure A1. Correlation heatmap of all 22 variables selected at the initial stage for Bundelkhand

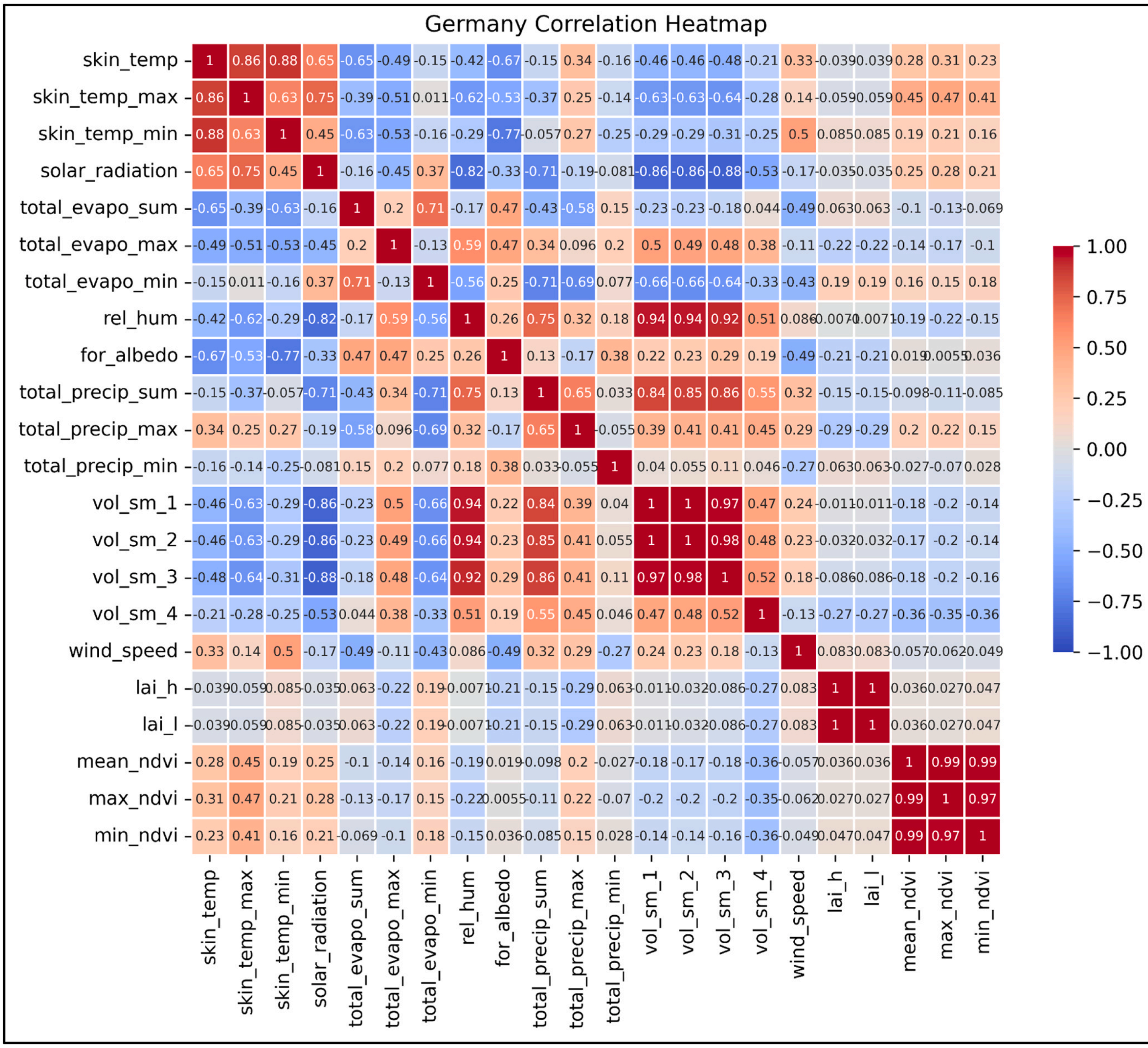

Figure A2. Correlation heatmap of all 22 variables selected at the initial stage for Germany

Appendix A. Supporting information

Supplementary data associated with this article can be found in the online version at doi:10.1016/j.agwat.2026.110254.

Data availability

Data will be made available on request.

References

Aalbers, E.E., Van Meijgaard, E., Lenderink, G., De Vries, H., Van Den Hurk, B.J.J.M., 2023. The 2018 west-central European drought projected in a warmer climate: how much drier can it get? Nat. Hazards Earth Syst. Sci. 23 (5), 1921–1946. https://doi.org/10.5194/NHESS-23-1921-2023.

Akbari, A., Ranjbar, A., Kazemzadeh, Y., Martyushev, D.A., 2025. Enhanced water saturation estimation in hydrocarbon reservoirs using machine learning. *2025 15:1* Sci. Rep. 15 (1), 29846. https://doi.org/10.1038/s41598-025-13982-5.

Alduchov, O.A., Eskridge, R.E., 1996. Improved Magnus Form Approximation of Saturation Vapor Pressure. J. Appl. Meteorol. Climatol. 35 (4), 601–609. https://doi.org/10.1175/1520-0450(1996)035<0601:IMFAOS>2.0.CO;2.

P. Anais (n.d.). *How to average winds*? Retrieved February 14, 2026, from ⟨https://help.marine.copernicus.eu/en/articles/5487266-how-to-average-winds⟩.

Ansarifar, J., Wang, L., Archontoulis, S.V., 2021. An interaction regression model for crop yield prediction. *2021 11:1* Sci. Rep. 11 (1), 17754. https://doi.org/10.1038/s41598-021-97221-7.

Arsenault, R., Brissette, F., Martel, J.L., 2018. The hazards of split-sample validation in hydrological model calibration. J. Hydrol. 566, 346–362. https://doi.org/10.1016/J.JHYDROL.2018.09.027.

Asadollah, S.B.H.S., Jodar-Abellan, A., Pardo, M.Á., 2024. Optimizing machine learning for agricultural productivity: A novel approach with RScv and remote sensing data over Europe. Agric. Syst. 218 (2), 103955. https://doi.org/10.1016/j.agsy.2024.103955.

Asfaw, D., Smith, R.G., Majumdar, S., Grote, K., Fang, B., Wilson, B.B., Lakshmi, V., Butler, J.J., 2025. Predicting groundwater withdrawals using machine learning with

limited metering data: Assessment of training data requirements. Agric. Water Manag. 318, 109691. https://doi.org/10.1016/J.AGWAT.2025.109691.
Baig, F., Ali, L., Faiz, M.A., Chen, H., Sherif, M., 2024. How accurate are the machine learning models in improving monthly rainfall prediction in hyper arid environment? J. Hydrol. 633, 131040. https://doi.org/10.1016/J.JHYDROL.2024.131040.
Beck, H.E., Zimmermann, N.E., McVicar, T.R., Vergopolan, N., Berg, A., Wood, E.F., 2018. Present and future Köppen-Geiger climate classification maps at 1-km resolution. Sci. Data 5. https://doi.org/10.1038/SDATA.2018.214.
Bellvert, J., Pamies-Sans, M., Casadesús, J., Girona, J., 2025. Evaluating the impact of drought and water restrictions on agricultural production in irrigated areas through crop water productivity functions and a remote sensing-based evapotranspiration model. Agric. Water Manag. 309, 109319. https://doi.org/10.1016/J.AGWAT.2025.109319.
Benito-Verdugo, P., Martínez-Fernández, J., González-Zamora, Á., Almendra-Martín, L., Gaona, J., Herrero-Jiménez, C.M., 2023. Impact of Agricultural Drought on Barley and Wheat Yield: A Comparative Case Study of Spain and Germany. Agric. (Switz.) 13 (11). https://doi.org/10.3390/agriculture13112111.
Benso, M.R., Silva, R.F., Chiquito Gesualdo, G., Saraiva, A.M., Delbem, A.C.B., Marques, P.A.A., Marengo, J.A., Mendiondo, E.M., 2025. A data-driven framework for assessing climatic impact drivers in the context of food security. Nat. Hazards Earth Syst. Sci. 25 (4), 1387–1404. https://doi.org/10.5194/NHESS-25-1387-2025.
Blickensdörfer, L., Schwieder, M., Pflugmacher, D., Nendel, C., Erasmi, S., Hostert, P., 2022. Mapping of crop types and crop sequences with combined time series of Sentinel-1, Sentinel-2 and Landsat 8 data for Germany. Remote Sens. Environ. 269, 112831. https://doi.org/10.1016/J.RSE.2021.112831.
Boeing, F., Rakovec, O., Kumar, R., Samaniego, L., Schrön, M., Hildebrandt, A., Rebmann, C., Thober, S., Müller, S., Zacharias, S., Bogena, H., Schneider, K., Kiese, R., Attinger, S., Marx, A., 2022. High-resolution drought simulations and comparison to soil moisture observations in Germany. Hydrol. Earth Syst. Sci. 26 (19), 5137–5161. https://doi.org/10.5194/hess-26-5137-2022.
Bourbour, H., Abdolahipour, M., Abdollahi, H., Abiar, E., Mashal, M., 2025. Pre-harvest forecasting of rainfed wheat yield in Iran using multi-source remote sensing and machine learning. Agric. Water Manag. 322, 110005. https://doi.org/10.1016/J.AGWAT.2025.110005.
Bowden, G.J., Maier, H.R., Dandy, G.C., 2002. Optimal division of data for neural network models in water resources applications. Water Resour. Res. 38 (2), 2-1–2–11. https://doi.org/10.1029/2001WR000266.
Brandt, P., Beyer, F., Borrmann, P., Möller, M., Gerighausen, H., 2024. Ensemble learning-based crop yield estimation: a scalable approach for supporting agricultural statistics. GIScience Remote Sens. 61 (1). https://doi.org/10.1080/15481603.2024.2367808.
Breiman, L., 2001. Random forests. Mach. Learn. 45 (1), 5–32. https://doi.org/10.1023/A:1010933404324.
Cai, Y., Guan, K., Lobell, D., Potgieter, A.B., Wang, S., Peng, J., Xu, T., Asseng, S., Zhang, Y., You, L., Peng, B., 2019. Integrating satellite and climate data to predict wheat yield in Australia using machine learning approaches. Agric. For. Meteorol. 274, 144–159. https://doi.org/10.1016/J.AGRFORMET.2019.03.010.
Cedric, L.S., Adoni, W.Y.H., Aworka, R., Zoueu, J.T., Mutombo, F.K., Krichen, M., Kimpolo, C.L.M., 2022. Crops yield prediction based on machine learning models: case of West African countries. Smart Agric. Technol. 2, 100049. https://doi.org/10.1016/J.ATECH.2022.100049.
Chen, J., Zheng, F., May, R., Guo, D., Gupta, H., Maier, H.R., 2022. Improved data splitting methods for data-driven hydrological model development based on a large number of catchment samples. J. Hydrol. 613, 128340. https://doi.org/10.1016/J.JHYDROL.2022.128340.
Dangare, P., Cronje, P.J.R., Mashimbye, Z.E., Masanganise, J., Ntshidi, Z., Gokool, S., Naiken, V., Sawunyama, T., Dzikiti, S., 2026. Modelling water - use and yield of selected irrigated subtropical crops using machine learning and hybrid models in north - eastern South Africa. Agric. Water Manag. 324, 110113. https://doi.org/10.1016/J.AGWAT.2025.110113.
De Clercq, D., Mahdi, A., 2024. Feasibility of machine learning-based rice yield prediction in India at the district level using climate reanalysis and remote sensing data. Agric. Syst. 220, 104099. https://doi.org/10.1016/J.AGSY.2024.104099.
DES | Area, Production & Yield - Reports. (n.d.). Retrieved May 5, 2025, from ⟨https://data.desagri.gov.in/website/crops-apy-report-web⟩.
Duden, C., Nacke, C., Offermann, F., 2024. German yield and area data for 11 crops from 1979 to 2021 at a harmonized spatial resolution of 397 districts. Sci. Data 11 (1), 1–10. https://doi.org/10.1038/S41597-024-02951-8.
El-Kenawy, E.S.M., Alhussan, A.A., Khodadadi, N., Mirjalili, S., Eid, M.M., 2024. Predicting Potato Crop Yield with Machine Learning and Deep Learning for Sustainable Agriculture. Potato Res. https://doi.org/10.1007/s11540-024-09753-w.
Ennaji, O., Hamma, A., Vergütz, L., El Allali, A., 2025. The assessment of soil variables relative importance for cereal yield prediction under rainfed cropping system in Morocco. Smart Agric. Technol. 11, 100950. https://doi.org/10.1016/J.ATECH.2025.100950.
ERA5-Land monthly averaged data from 1950 to present. (n.d.). Retrieved May 5, 2025, from ⟨https://cds.climate.copernicus.eu/datasets/reanalysis-era5-land-monthly-means?tab=download⟩.
Fares, A., Veettil, A.V., Rahman, A., Awal, R., 2026. A review of artificial intelligence applications for predicting crop performance and enhancing food security under drought-induced water stress. Agric. Water Manag. 325 (12), 110212. https://doi.org/10.1016/j.agwat.2026.110212.
Gallear, J.W., Valadares Galdos, M., Zeri, M., Hartley, A., 2025. Evaluation of machine learning approaches for large-scale agricultural drought forecasts to improve monitoring and preparedness in Brazil. Nat. Hazards Earth Syst. Sci. 25 (4), 1521–1541. https://doi.org/10.5194/NHESS-25-1521-2025.
Gao, X., Liu, J., Lin, H., Javed, T., Yin, F., Chen, R., Wen, Y., Zhang, J., Yi, K., Wang, Z., 2025. Using machine learning techniques to evaluate the impact of future climate change on wheat yields in Xinjiang, China. Agric. Water Manag. 317, 109646. https://doi.org/10.1016/j.agwat.2025.109646.
Garg, S., Dasgupta, A., Motagh, M., Martinis, S., Selvakumaran, S., 2024. Unlocking the full potential of Sentinel-1 for flood detection in arid regions. Remote Sens. Environ. 315, 114417. https://doi.org/10.1016/J.RSE.2024.114417.
Han, L., Leng, G., 2024. Significant changes in global maize yield sensitivity to vapor pressure deficit during 1983–2010. Agric. Water Manag. 305, 109107. https://doi.org/10.1016/J.AGWAT.2024.109107.
Hauswirth, S.M., Bierkens, M.F.P., Beijk, V., Wanders, N., 2021. The potential of data driven approaches for quantifying hydrological extremes. Adv. Water Resour. 155, 104017. https://doi.org/10.1016/J.ADVWATRES.2021.104017.
Hoppe, H., Dietrich, P., Marzahn, P., Weiß, T., Nitzsche, C., Freiherr von Lukas, U., Wengerek, T., Borg, E., 2024. Transferability of Machine Learning Models for Crop Classification in Remote Sensing Imagery Using a New Test Methodology: A Study on Phenological, Temporal, and Spatial Influences. Vol. 16, 1493 Remote Sens. 2024 16 (9), 1493. https://doi.org/10.3390/RS16091493.
ICRISAT-District Level Data. (n.d.). Retrieved May 5, 2025, from ⟨http://data.icrisat.org/dld/src/crops.html⟩.
India Meteorological Department. (2020). *ANNUAL REPORT 2019*. ⟨https://metnet.imd.gov.in/docs/imdnews/ANNUAL_REPORT2019English.pdf⟩.
Jhajharia, K., Mathur, P., Jain, S., Nijhawan, S., 2023. Crop Yield Prediction using Machine Learning and Deep Learning Techniques. Procedia Comput. Sci. 218, 406–417. https://doi.org/10.1016/J.PROCS.2023.01.023.
Johnston, D.B., Pembleton, K.G., Huth, N.I., Deo, R.C., 2023. Comparison of machine learning methods emulating process driven crop models. Environ. Model. Softw. 162 (2), 105634. https://doi.org/10.1016/j.envsoft.2023.105634.
Joshi, A., Pradhan, B., Chakraborty, S., Behera, M.D., 2023. Winter wheat yield prediction in the conterminous United States using solar-induced chlorophyll fluorescence data and XGBoost and random forest algorithm. Ecol. Inform. 77, 102194. https://doi.org/10.1016/J.ECOINF.2023.102194.
Khan, S.N., Li, D., Maimaitijiang, M., 2024. Using gross primary production data and deep transfer learning for crop yield prediction in the US Corn Belt. Int. J. Appl. Earth Obs. Geoinf. 131, 103965. https://doi.org/10.1016/J.JAG.2024.103965.
Khechba, K., Belgiu, M., Laamrani, A., Stein, A., Amazirh, A., Chehbouni, A., 2025. The impact of spatiotemporal variability of environmental conditions on wheat yield forecasting using remote sensing data and machine learning. Int. J. Appl. Earth Obs. Geoinf. 136, 104367. https://doi.org/10.1016/J.JAG.2025.104367.
Khosravani Shariati, S.A., Abbasi, A., 2025. Machine learning-based winter wheat yield prediction using multisource data. Agric. Water Manag. 322 (33), 109951. https://doi.org/10.1016/j.agwat.2025.109951.
Kratzert, F., Klotz, D., Herrnegger, M., Sampson, A.K., Hochreiter, S., Nearing, G.S., 2019. Toward Improved Predictions in Ungauged Basins: Exploiting the Power of Machine Learning. Water Resour. Res. 55 (12), 11344–11354. https://doi.org/10.1029/2019WR026065.
Kundu, A., Mario Denis, D., Patel, N.R., 2015. Evaluation of the meteorological drought over the Bundelkhand region using geo-spatial techniques. Clim. Change 1 (4), 418–424. ⟨https://discoveryjournals.org/climate_change/current_issue/v1/n4/A13.pdf⟩.
Lei, C., Chen, J., Ibáñez, I., Sciusco, P., Shirkey, G., Lei, M., Reich, P., Robertson, G.P., 2024. Albedo of crops as a nature-based climate solution to global warming. Environ. Res. Lett. 19 (8), 084032. https://doi.org/10.1088/1748-9326/AD5FA2.
Leng, G., Hall, J.W., 2020. Predicting spatial and temporal variability in crop yields: an inter-comparison of machine learning, regression and process-based models. Environ. Res. Lett. 15 (4), 044027. https://doi.org/10.1088/1748-9326/AB7B24.
Li, M., Cao, S., Zhu, Z., Wang, Z., Myneni, R.B., Piao, S., 2023a. Spatiotemporally consistent global dataset of the GIMMS Normalized Difference Vegetation Index (PKU GIMMS NDVI) from 1982 to 2022. Earth Syst. Sci. Data 15 (9), 4181–4203. https://doi.org/10.5194/ESSD-15-4181-2023.
Li, L., He, Q., Harrison, M.T., Shi, Y., Feng, P., Wang, B., Zhang, Y., Li, Y., Liu, D.L., Yang, G., Zhou, M., Yu, Q., Liu, K., 2025. Knowledge-guided machine learning for improving crop yield projections of waterlogging effects under climate change. Resour. Environ. Sustain. 19, 100185. https://doi.org/10.1016/J.RESENV.2024.100185.
Li, X., Jin, H., Eklundh, L., Houssaine Bouras, E., Olsson, P.O., Cai, Z., Ardö, J., Duan, Z., 2024. Estimation of district-level spring barley yield in southern Sweden using multi-source satellite data and random forest approach. Int. J. Appl. Earth Obs. Geoinf. 134. https://doi.org/10.1016/j.jag.2024.104183.
Li, Y., Zeng, H., Zhang, M., Wu, B., Zhao, Y., Yao, X., Cheng, T., Qin, X., Wu, F., 2023b. A county-level soybean yield prediction framework coupled with XGBoost and multidimensional feature engineering. Int. J. Appl. Earth Obs. Geoinf. 118, 103269. https://doi.org/10.1016/J.JAG.2023.103269.
Luo, L., Sun, S., Xue, J., Gao, Z., Zhao, J., Yin, Y., Gao, F., Luan, X., 2023. Crop yield estimation based on assimilation of crop models and remote sensing data: A systematic evaluation. Agric. Syst. 210 (2), 103711. https://doi.org/10.1016/j.agsy.2023.103711.
Mahdizadeh Gharakhanlou, N., Perez, L., 2024. From data to harvest: Leveraging ensemble machine learning for enhanced crop yield predictions across Canada amidst climate change. Sci. Total Environ. 951, 175764. https://doi.org/10.1016/J.SCITOTENV.2024.175764.
Maier, H.R., Zheng, F., Gupta, H., Chen, J., Mai, J., Savic, D., Loritz, R., Wu, W., Guo, D., Bennett, A., Jakeman, A., Razavi, S., Zhao, J., 2023. On how data are partitioned in model development and evaluation: Confronting the elephant in the room to

enhance model generalization. Environ. Model. Softw. 167, 105779. https://doi.org/10.1016/J.ENVSOFT.2023.105779.
Mishra, A.K., Singh, V.P., 2010. A review of drought concepts. J. Hydrol. 391 (Numbers 1–2), 202–216. https://doi.org/10.1016/j.jhydrol.2010.07.012.
Muñoz-Sabater, J., Dutra, E., Agustí-Panareda, A., Albergel, C., Arduini, G., Balsamo, G., Boussetta, S., Choulga, M., Harrigan, S., Hersbach, H., Martens, B., Miralles, D.G., Piles, M., Rodríguez-Fernández, N.J., Zsoter, E., Buontempo, C., Thépaut, J.N., 2021. ERA5-Land: A state-of-the-art global reanalysis dataset for land applications. Earth Syst. Sci. Data 13 (9), 4349–4383. https://doi.org/10.5194/ESSD-13-4349-2021.
Muyi Li, Sen Cao, Zaichun Zhu, Zhe Wang, Ranga B. Myneni, & Shilong Piao. (2023, August 17). *GIMMS Normalized Difference Vegetation Index 1982-2022*. ⟨https://zenodo.org/records/8253971⟩.
Nevavuori, P., Narra, N., Lipping, T., 2019. Crop yield prediction with deep convolutional neural networks. Comput. Electron. Agric. 163, 104859. https://doi.org/10.1016/J.COMPAG.2019.104859.
Orynbaikyzy, A., Gessner, U., Conrad, C., 2022. Spatial Transferability of Random Forest Models for Crop Type Classification Using Sentinel-1 and Sentinel-2. Remote Sens. 14 (6), 1493. https://doi.org/10.3390/rs14061493.
Pandey, V., Srivastava, P.K., Singh, S.K., Petropoulos, G.P., Mall, R.K., 2021. Drought Identification and Trend Analysis Using Long-Term CHIRPS Satellite Precipitation Product in Bundelkhand, India. Vol. 13, 1042 Sustainability 2021 13 (3), 1042. https://doi.org/10.3390/SU13031042.
Patel, N.R., Yadav, K., 2015. Monitoring spatio-temporal pattern of drought stress using integrated drought index over Bundelkhand region, India. Nat. Hazards 77 (2), 663–677. https://doi.org/10.1007/s11069-015-1614-0.
Paul, S., Mridha, N., Vellaichamy, S., Singh, P., 2021. Development of a composite measure for mapping rural food and nutrition security: application and validation in the drought-prone Bundelkhand region of India. Food Secur. 13 (3), 617–635. https://doi.org/10.1007/S12571-021-01152-0.
Peng, B., Guan, K., Zhou, W., Jiang, C., Frankenberg, C., Sun, Y., He, L., Köhler, P., 2020. Assessing the benefit of satellite-based Solar-Induced Chlorophyll Fluorescence in crop yield prediction. Int. J. Appl. Earth Obs. Geoinf. 90. https://doi.org/10.1016/j.jag.2020.102126.
Qian, T., Su, X., Wu, H., Singh, V.P., Zhang, T., 2025. An agricultural drought early warning threshold model with considering copula combined with diminishing marginal benefit theory: A case study in the Yellow River basin. Agric. Water Manag. 316, 109582. https://doi.org/10.1016/J.AGWAT.2025.109582.
Reinermann, S., Gessner, U., Asam, S., Kuenzer, C., Dech, S., 2019. The Effect of Droughts on Vegetation Condition in Germany: An Analysis Based on Two Decades of Satellite Earth Observation Time Series and Crop Yield Statistics. Vol. 11, 1783 Remote Sens. 2019 11 (15), 1783. https://doi.org/10.3390/RS11151783.
Roberts, D.R., Bahn, V., Ciuti, S., Boyce, M.S., Elith, J., Guillera-Arroita, G., Hauenstein, S., Lahoz-Monfort, J.J., Schröder, B., Thuiller, W., Warton, D.I., Wintle, B.A., Hartig, F., Dormann, C.F., 2017. Cross-validation strategies for data with temporal, spatial, hierarchical, or phylogenetic structure. Ecography 40 (8), 913–929. https://doi.org/10.1111/ECOG.02881.
Ruan, G., Li, X., Yuan, F., Cammarano, D., Ata-UI-Karim, S.T., Liu, X., Tian, Y., Zhu, Y., Cao, W., Cao, Q., 2022. Improving wheat yield prediction integrating proximal sensing and weather data with machine learning. Comput. Electron. Agric. 195, 106852. https://doi.org/10.1016/J.COMPAG.2022.106852.
Sahu, H., Garg, P.K., Vijay, S., Dasgupta, A., 2025a. Annu. Crop Yield Predict. Using AI EO 5760–5763. https://doi.org/10.1109/IGARSS55030.2025.11243362.
Sahu, H., Garg, P.K., Vijay, S., Dasgupta, A., 2025b. Estimating drought impacts on crop yield using AI and EO. EGU 25. https://doi.org/10.5194/EGUSPHERE-EGU25-2768.
Samaniego, L., Kumar, R., Zink, M., Samaniego, L., Kumar, R., Zink, M., 2013. Implications of Parameter Uncertainty on Soil Moisture Drought Analysis in Germany. J. Hydrometeorol. 14 (1), 47–68. https://doi.org/10.1175/JHM-D-12-075.1.
Sánchez, J.C.M., Mesa, H.G.A., Espinosa, A.T., Castilla, S.R., Lamont, F.G., 2025. Improving wheat yield prediction through variable selection using Support Vector Regression, Random Forest, and Extreme Gradient Boosting. Smart Agric. Technol. 10, 100791. https://doi.org/10.1016/J.ATECH.2025.100791.
Saravanan, K.S., Bhagavathiappan, V., 2024. Prediction of crop yield in India using machine learning and hybrid deep learning models. *72:6* Acta Geophys. 2024 72 (6), 4613–4632. https://doi.org/10.1007/S11600-024-01312-8.
Schmitt, J., Offermann, F., Söder, M., Frühauf, C., Finger, R., 2022. Extreme weather events cause significant crop yield losses at the farm level in German agriculture. Food Policy 112, 102359. https://doi.org/10.1016/J.FOODPOL.2022.102359.
Schwarz, M., Landmann, T., Cornish, N., Wetzel, K.F., Siebert, S., Franke, J., 2020. A spatially transferable drought hazard and drought risk modeling approach based on remote sensing data. Vol. 12, 237 Remote Sens. 2020 12 (2), 237. https://doi.org/10.3390/RS12020237.
Servia, H., Pareeth, S., Michailovsky, C.I., de Fraiture, C., Karimi, P., 2022. Operational framework to predict field level crop biomass using remote sensing and data driven models. Int. J. Appl. Earth Obs. Geoinf. 108. https://doi.org/10.1016/j.jag.2022.102725.
Seyedmohammadi, J., Navidi, M.N., Zeinadini, A., McDowell, R.W., 2024. Random forest, an efficient smart technique for analyzing the influence of soil properties on pistachio yield. Environ. Dev. Sustain. 26 (1), 2615–2636. https://doi.org/10.1007/S10668-023-03926-2.
Shahhosseini, M., Hu, G., Huber, I., Archontoulis, S.V., 2021. Coupling machine learning and crop modeling improves crop yield prediction in the US Corn Belt. *2021 11:1* Sci. Rep. 11 (1), 1606. https://doi.org/10.1038/s41598-020-80820-1.
Sharafi, S., Nahvinia, M.J., 2024. Sustainability insights: enhancing rainfed wheat and barley yield prediction in arid regions. Agric. Water Manag. 299. https://doi.org/10.1016/j.agwat.2024.108857.
Shi, Y., Li, L., Wu, B., Zhang, Y., Wang, B., Niu, W., He, L., Jin, N., Pan, S., Tian, H., Yu, Q., 2024. Predicting rice productivity for ground data-sparse regions: A transferable framework and its application to North Korea. Sci. Total Environ. 946, 174227. https://doi.org/10.1016/J.SCITOTENV.2024.174227.
Stagge, J.H., Sung, K., Munyejuru, I.F., Haidar, M.A.I., 2025. Expected annual minima from an idealized moving-average drought index. Hydrol. Earth Syst. Sci. 29 (3), 719–732. https://doi.org/10.5194/HESS-29-719-2025.
Su, Z., Yu, Z., Gu, Z., Zhao, D., Peng, J., 2025. Unravelling the hidden drivers of crop sensitivity to precipitation in the arid and semi-arid regions of Northwest China. Agric. Water Manag. 320, 109866. https://doi.org/10.1016/j.agwat.2025.109866.
Sweet, L., Müller, C., Anand, M., Zscheischler, J., 2023. Cross-validation strategy impacts the performance and interpretation of machine learning models. Artif. Intell. Earth Syst. 2 (4). https://doi.org/10.1175/AIES-D-23-0026.1.
Tanguy, M., Eastman, M., Magee, E., Barker, L.J., Chitson, T., Ekkawatpanit, C., Goodwin, D., Hannaford, J., Holman, I., Pardthaisong, L., Parry, S., Rey Vicario, D., Visessri, S., 2023. Indicator-to-impact links to help improve agricultural drought preparedness in Thailand. Nat. Hazards Earth Syst. Sci. 23 (7), 2419–2441. https://doi.org/10.5194/NHESS-23-2419-2023.
Tegegne, G., Park, D.K., Kim, Y.O., 2017. Comparison of hydrological models for the assessment of water resources in a data-scarce region, the Upper Blue Nile River Basin. J. Hydrol. Reg. Stud. 14, 49–66. https://doi.org/10.1016/J.EJRH.2017.10.002.
Tramblay, Y., Quintana Seguí, P., 2022. Estimating soil moisture conditions for drought monitoring with random forests and a simple soil moisture accounting scheme. Nat. Hazards Earth Syst. Sci. 22 (4), 1325–1334. https://doi.org/10.5194/nhess-22-1325-2022.
UFZ-Germany. (n.d.). *Droughts* 1952 - 2024. Retrieved May 5, 2025, from ⟨https://www.ufz.de/index.php?de=47252⟩.
Uttar Pradesh Government. (2023). *Uttar Pradesh: State Disaster Management Plan-2023 (Part-1)*. ⟨https://upsdma.up.nic.in/2023/SDMP-Plan-Part-1.pdf⟩.
van der Wiel, K., Batelaan, T.J., Wanders, N., 2022. Large increases of multi-year droughts in north-western Europe in a warmer climate. Clim. Dyn. 60 (5), 1781–1800. https://doi.org/10.1007/S00382-022-06373-3, 2022 60:5.
van Klompenburg, T., Kassahun, A., Catal, C., 2020. Crop yield prediction using machine learning: A systematic literature review. Comput. Electron. Agric. 177, 105709. https://doi.org/10.1016/J.COMPAG.2020.105709.
Verschuur, J., Li, S., Wolski, P., Otto, F.E.L., 2021. Climate change as a driver of food insecurity in the 2007 Lesotho-South Africa drought. Sci. Rep. 11 (1). https://doi.org/10.1038/s41598-021-83375-x.
Wan, W., Liu, Z., Li, K., Wang, G., Wu, H., Wang, Q., 2021. Drought monitoring of the maize planting areas in Northeast and North China Plain. Agric. Water Manag. 245. https://doi.org/10.1016/j.agwat.2020.106636.
Wang, Y.Q., Leng, P., Shang, G.F., Zhang, X., Li, Z.L., 2023b. Sun-induced chlorophyll fluorescence is superior to satellite vegetation indices for predicting summer maize yield under drought conditions. Comput. Electron. Agric. 205, 107615. https://doi.org/10.1016/J.COMPAG.2023.107615.
Wang, Y., Shi, W., Wen, T., 2023a. Prediction of winter wheat yield and dry matter in North China Plain using machine learning algorithms for optimal water and nitrogen application. Agric. Water Manag. 277, 108140. https://doi.org/10.1016/J.AGWAT.2023.108140.
Webber, H., Lischeid, G., Sommer, M., Finger, R., Nendel, C., Gaiser, T., Ewert, F., 2020. No perfect storm for crop yield failure in Germany. Environ. Res. Lett. 15 (10). https://doi.org/10.1088/1748-9326/aba2a4.
Wen, W., Timmermans, J., Chen, Q., van Bodegom, P.M., 2023. Evaluating crop-specific responses to salinity and drought stress from remote sensing. Int. J. Appl. Earth Obs. Geoinf. 122. https://doi.org/10.1016/j.jag.2023.103438.
Xu, Y., Albalawneh, A., Al-Zoubi, M., Baroud, H., 2025. Variance-based sensitivity analysis of climate variability impact on crop yield using machine learning: A case study in Jordan. Agric. Water Manag. 313, 109409. https://doi.org/10.1016/J.AGWAT.2025.109409.
Yeşilköy, S., Demir, I., 2024. Crop yield prediction based on reanalysis and crop phenology data in the agroclimatic zones. Theor. Appl. Climatol. 155 (7), 7035–7048. https://doi.org/10.1007/s00704-024-05046-x.
Zhang, B., Abu Salem, F.K., Hayes, M.J., Smith, K.H., Tadesse, T., Wardlow, B.D., 2023. Explainable machine learning for the prediction and assessment of complex drought impacts. Sci. Total Environ. 898, 165509. https://doi.org/10.1016/J.SCITOTENV.2023.165509.
Zhang, J., Campana, P.E., Yao, T., Zhang, Y., Lundblad, A., Melton, F., Yan, J., 2018. The water-food-energy nexus optimization approach to combat agricultural drought: a case study in the United States. Appl. Energy 227, 449–464. https://doi.org/10.1016/j.apenergy.2017.07.036.
Zhang, Y., Wang, P., Li, Y., Han, D., Wu, D., Liu, S., Guo, J., 2025. A quantification method for cumulative drought effects on summer maize yield incorporating recovery dynamics based on Vegetation Water Index. Agric. Water Manag. 320, 109865. https://doi.org/10.1016/J.AGWAT.2025.109865.
Zhao, W., Wu, H., Yin, G., Duan, S.-B., 2019. Normalization of the temporal effect on the MODIS land surface temperature product using random forest regression. ISPRS J. Photogramm. Remote Sens. 152, 109–118. https://doi.org/10.1016/j.isprsjprs.2019.04.008. ISSN 0924-2716.
Zhou, Z., Yu, L., Zhang, Y., Jia, B., Zhang, L., Luo, S., 2025. Cascade reservoir outflow simulation based on physics-constrained random forest. Water (Switz.) 17 (14), 2154. https://doi.org/10.3390/w17142154.
Zhuo, W., Fang, S., Gao, X., Wang, L., Wu, D., Fu, S., Wu, Q., Huang, J., 2022. Crop yield prediction using MODIS LAI, TIGGE weather forecasts and WOFOST model: a case study for winter wheat in Hebei, China during 2009–2013. Int. J. Appl. Earth Obs. Geoinf. 106. https://doi.org/10.1016/j.jag.2021.102668.